ETH
Eidgenössische Technische Hochschule Zürich
Swiss Federal Institute of Technology Zurich

Seminar for Applied Mathematics SAM

Uncertainty quantification for hyperbolic systems of conservation laws

R. Abgrall and S. Mishra

Research Report No. 2016-58
December 2016

Seminar für Angewandte Mathematik
Eidgenössische Technische Hochschule
CH-8092 Zürich
Switzerland

Funding ERC: 306279 SPARCCLE
To appear in the Handbook of Numerical Analysis: Hyperbolic problems.

Uncertainty quantification for hyperbolic systems of conservation laws

R. Abgrall [*], and S. Mishra [†]

December 18, 2016

Abstract

We review uncertainty quantification (UQ) for hyperbolic systems of conservation (balance) laws. The input uncertainty could be in the initial data, fluxes, coefficients, source terms or boundary conditions. We focus on forward UQ or uncertainty propagation and review deterministic methods such as stochastic Galerkin and stochastic collocation finite volume methods for approximating random (field) entropy solutions. Statistical sampling methods of the Monte Carlo and Multi-level Monte Carlo (MLMC) type, are also described. We present alternative UQ frameworks such as measure valued solutions and statistical solutions.

1 Introduction

Systems of balance laws are nonlinear partial differential equations of the generic form

$$\partial_t \mathbf{U} + \nabla_x \cdot \mathbf{F}(\mathbf{c}(x,t), \mathbf{U}) = \mathbf{S}(x,t,\mathbf{U}), \tag{1.1a}$$

$$\mathbf{U}(x,0) = \mathbf{U}_0(x). \tag{1.1b}$$

Here, the unknown $\mathbf{U} = \mathbf{U}(x,t) : \mathbb{R}^d \times \mathbb{R}_+ \to \mathbb{R}^N$ is the vector of *conserved variables*, $\mathbf{F} = (\mathbf{F}^1, \ldots, \mathbf{F}^d) : \mathbb{R}^{N\times N} \to \mathbb{R}^{N\times d}$ is the *flux function*, $\mathbf{c} = (\mathbf{c}^1, \ldots, \mathbf{c}^d) : \mathbb{R}^d \times \mathbb{R}_+ \to \mathbb{R}^{N\times d}$ is a spatio-temporal coefficient and $\mathbf{S} : \mathbb{R}^d \times \mathbb{R}_+ \times \mathbb{R}^N \to \mathbb{R}^N$ is a source (sink) term. We denote $\mathbb{R}_+ := [0, \infty)$. Here, $\mathbf{U}_0$ denotes the prescribed initial data. Furthermore, the system needs to be supplemented with suitable boundary conditions.

The system (1.1) is termed a *conservation law* if $\mathbf{S} \equiv 0$. It is termed *hyperbolic* if the flux Jacobian matrix has real eigenvalues [15]. Hyperbolic systems of conservation (balance) laws arise in a wide variety of models in physics and engineering. Prototypical examples include the compressible Euler equations of gas dynamics, the shallow water equations of oceanography, the magneto-hydrodynamics (MHD) equations of plasma physics and the equations of nonlinear elasticity [15].

It is well known that solutions of (1.1) develop discontinuities in finite time, even when the initial data is smooth [15]. Hence, solutions of (1.1) are sought (and computed) in the weak sense: a weak solution $\mathbf{U} \in (L^1_{\text{loc}}(\mathbb{R}^d \times \mathbb{R}_+))^N$ is required to satisfy the integral identity

$$\int_{R_+}\int_{R^d} \left(\mathbf{U}\varphi_t + \sum_{j=1}^{d} \mathbf{F}^j(\mathbf{c}^j, \mathbf{U})\varphi_{x_j} + \mathbf{S}(x,t,\mathbf{U})\varphi \right) dxdt + \int_{R^d} \mathbf{U}_0(x)\varphi(x,0)dx = 0\,, \tag{1.2}$$

for all test functions $\varphi \in C^1_0(\mathbb{R}_+ \times \mathbb{R}^d)$. It is well known that weak solutions are not necessarily unique [15]. Additional admissibility criteria or *entropy conditions* are necessary to obtain uniqueness. In space dimension $d > 1$, rigorous existence and uniqueness results for conservation (balance) laws and for generic initial data are available only for the scalar case, i.e, in the case $N = 1$.

[*]Institute of Mathematics, University of Zürich, Switzerland

[†]Seminar for Applied Mathematics, ETH Zürich, Rämistrasse 101, Zürich, Switzerland.

1.1 Numerical methods.

Numerical schemes have assumed the role of being the main tools for the study of systems of balance (conservation) laws. Many efficient numerical schemes for approximating systems of conservation laws are currently available. They include the Finite Volume, conservative Finite Difference, Discontinuous Galerkin finite element methods Continuous Statbilized Finite Element Methods and Residual Distribution methods, see [61, 20, 74, 11, 9]. For simplicity of exposition and to fix notation, we present the standard Finite Volume Method (FVM) [20].

We consider here a triangulation $\mathcal{T}$ of the spatial domain $D \subset \mathbb{R}^d$ of interest. Here, the term triangulation $\mathcal{T}$ will be understood as a partition of the physical domain into a finite set of disjoint open, convex polyhedra $K \subset \mathbb{R}^d$ with boundary ∂K being a finite union of closed, plane faces (which are polyhedra contained in $d-1$ dimensional hyperplanes, understood as points in the case $d = 1$). Let $\Delta x_K := \operatorname{diam} K = \sup\{|x - y| : x, y \in K\}$ and by $\Delta x(\mathcal{T}) := \max\{\Delta x_K : K \in \mathcal{T}\}$ denote the *mesh width* of the underlying triangulation. For any volume $K \in \mathcal{T}$, we define the *set* $\mathcal{N}(K)$ *of neighbouring volumes*

$$\mathcal{N}(K) := \{K' \in \mathcal{T} : K' \neq K \text{ and } \operatorname{meas}_{d-1}(\overline{K} \cap \overline{K'}) > 0\}. \tag{1.3}$$

For every $K \in \mathcal{T}$ and $K' \in \mathcal{N}(K)$ denote $\mathbf{n}_{K,K'}$ to be the exterior unit normal vector, i.e. pointing outward from the volume K at the face $\overline{K} \cap \overline{K'}$. We set:

$$\lambda_n = \Delta t^n / \min\{\Delta x_K : K \in \mathcal{T}\} \tag{1.4}$$

by denoting Δt^n as the n-th time step. The constant λ is determined by a standard CFL condition (see [20]) based on the maximum wave speed at the underlying time step.

Then, an explicit first-order finite volume ([20]) for approximating (1.1) is given by

$$\mathbf{U}_K^{n+1} = \mathbf{U}_K^n - \frac{\Delta t^n}{\operatorname{meas}(K)} \sum_{K' \in \mathcal{N}(K)} \mathbf{F}(\mathbf{c}_K^n, \mathbf{U}_K^n, \mathbf{c}_{K'}^n, \mathbf{U}_{K'}^n) + \Delta t^n \mathbf{S}_K^n, \tag{1.5}$$

where

$$\mathbf{U}_K^n \approx \frac{1}{\operatorname{meas}(K)} \int_K \mathbf{U}(x, t^n) dx$$

is an approximation to the cell average of the solution, $\mathbf{c}_K^n$ is similarly the average of the coefficient $\mathbf{c}$ in the cell K and $\mathbf{F}(\cdot,\cdot,\cdot,\cdot)$ is a numerical flux that is consistent with $\mathbf{F}(\mathbf{c}, \mathbf{U}) \cdot \mathbf{n}_{K,K'}$. Numerical fluxes are usually derived by (approximately) solving Riemann problems at each cell edge resulting in the Godunov, Roe and HLL fluxes, see [61]. The discrete source $\mathbf{S}$ in (1.5) can be a straight-forward evaluation,

$$\mathbf{S}_K^n = \frac{1}{\operatorname{meas}(K)} \int_K \mathbf{S}(x, t, \mathbf{U}_K^n) dx$$

or something more sophisticated, for instance the well-balanced version of the bottom topography source term [79] in shallow-water simulations, or the inclusion of the source term directly in the terms to update the solution as in Residual Distribution methods [40].

Higher order spatial accuracy is obtained by reconstructing $\mathbf{U}$ from $\mathbf{U}_K^n$ in terms of non-oscillatory piecewise polynomial functions, within the TVD [61], ENO [6] and WENO [14] procedures or using Discontinuous Galerkin methods (see, e.g. [10]). Higher order temporal accuracy can be achieved by employing strong stability preserving Runge-Kutta methods [1]. Space-time DG-discretizations can also be employed for uniformly high-order spatio-temporal accuracy [7]. We refer the reader to other chapters in this handbook for a detailed description of the state of the art numerical methods for systems of conservation (balance) laws.

1.2 Uncertainty Quantification (UQ)

Any numerical scheme approximating (1.1) requires the initial data $\mathbf{U}_0$, the source term $\mathbf{S}$, the coefficients $\mathbf{c}$ and the flux function $\mathbf{F}$, as well as suitable boundary conditions, as inputs. However, in practice, these inputs are obtained by measurements (observations). However, measurements cannot be precise and always involve some degree of uncertainty.

As a first example, consider the modeling of propagation of tsunami waves with the shallow water equations. It is not always possible to measure the initial water displacement (at tsunami source) with any precision in

real time, particularly for earthquake generated tsunamis. The Okada model that is usually employed to convert earthquake fault intensity into initial wave displacements consists of many uncertain parameters. Similarly, the bottom topography is measured with sonar equipment and this data collection can be prone to uncertainty. Thus, the inputs (initial data, flux coefficients and source terms) to the underlying shallow water equations are uncertain. As a second example, consider the modeling of an oil and gas reservoir. Water flooding is modeled by the equations of two phase flow. However, the rock permeability as well as the relative permeabilities of each phase with respect to the other, need to be measured. Again, the measurement process is characterized by uncertainty. Consequently, the inputs (the fluxes) to the underlying two-phase flow equations are uncertain. As a final motivating example, consider the flow past an aerofoil, or a full aircraft wing. The inputs to this calculation, such as the inflow Mach number and angle of attack as well as the parameters that specify the aerofoil geometry are all measured with some uncertainty.

This uncertainty in the inputs for (1.1) results in the propagation of uncertainty in the solution. The modeling and approximation of the propagation of uncertainty in the solution due to uncertainty in inputs constitutes the theme of uncertainty quantification (UQ).

UQ is a rapidly emerging interdisciplinary research area that spans applied mathematics, scientific computing, statistics and engineering. Although UQ involves various aspects in the modeling and computation of uncertainty, we focus on the rather limited aspect of *computational uncertainty propagation* here. Uncertainty propagation, also called *forward UQ*, refers to the computation of solutions of PDEs with uncertain inputs such as initial data, boundary conditions, coefficients, source terms etc. Given our focus on nonlinear hyperbolic PDEs, we shall discuss forward UQ in the limited context of systems of conservation (balance) laws (1.1). The reader is referred to [58] for a comprehensive discussion of UQ in the context of elliptic, parabolic and linear hyperbolic PDEs.

It is a non-trivial matter to develop efficient algorithms for quantifying uncertainty in solutions of conservation (balance) laws with random inputs. One of the main challenges lies in the fact that discontinuities in physical space (which inevitably arise in solutions of hyperbolic conservation laws) may propagate into parametric representations of the probability densities (laws) of the resulting random solutions. A robust numerical method should be able to deal with this phenomenon. Another challenge lies in dealing with the fact that the number of random sources driving the uncertainty may be very large (possibly countably infinite in the case of random field inputs parametrized by Karhunen-Loeve or other spectral representation).

The design of efficient numerical schemes for quantifying uncertainty in solutions of partial differential equations has seen a lot of activity in recent years, see [27] for a detailed review. Our main aim in this chapter is to review this activity in a condensed manner. We will describe modeling uncertain inputs (and resulting solutions) with random fields in section 2. We group proposed methods for UQ for hyperbolic systems in three broad categories. The first category of so-called *stochastic Galerkin* methods are described in section 3. The second category of methods, which we arrange under the label of *stochastic collocation* methods are presented in section 4 and the last category of Monte-Carlo type methods are described in section 5. We discuss the comparative advantages and disadvantages of each category of methods. The vexing issue of well-posedness of the underlying random conservation laws and rigorous convergence results for UQ algorithms, partially stems from representing solutions as random fields. An alternative approach, based on statistical solutions has been proposed very recently [77]. We briefly review this solution paradigm and the corresponding UQ algorithms for simulating it in section 6.

2 Random fields and random entropy solutions.

Let $(\Omega, \mathcal{F})$ be a measurable space, with Ω denoting the set of all elementary events, and $\mathcal{F}$ a σ-algebra of all possible events in our probability model. If $(E, \mathcal{G})$ denotes a second measurable space, then an *E-valued random variable* is any mapping $X : \Omega \to E$ such that the set $\{\omega \in \Omega\colon\ X(\omega) \in A\} \in \mathcal{F}$ for any $A \in \mathcal{G}$, i.e. X is a $\mathcal{G}$-measurable mapping from Ω into E.

We always assume that E is a metric space; with the Borel σ-field $\mathcal{B}(E)$, $(E, \mathcal{B}(E))$ is a measurable space and we shall assume that E-valued random variables $X : \Omega \to E$ will be $(\mathcal{F}, \mathcal{B}(E))$ measurable.

A probability measure $\mathbb{P}$ on $(\Omega, \mathcal{F})$ is any σ-additive set function from Ω into $[0, 1]$ such that $\mathbb{P}(\Omega) = 1$, and the measure space $(\Omega, \mathcal{F}, \mathbb{P})$ is called probability space. We shall always assume that $(\Omega, \mathcal{F}, \mathbb{P})$ is complete.

By $L^1(\Omega, \mathcal{F}, \mathbb{P}; E)$ we denote the set of all (equivalence classes of) integrable, E-valued random variables X. We equip it with the norm

$$\|X\|_{L^1(\Omega;E)} = \int_\Omega \|X(\Omega)\|_E \, \mathbb{P}(d\Omega) = \mathbb{E}(\|X\|_E) \ . \tag{2.1}$$

More generally, for $1 \leqslant p < \infty$, we define $L^p(\Omega, \mathcal{F}, \mathbb{P}; E)$ as the set of p-summable random variables taking values E and equip it with norm

$$\|X\|_{L^p(\Omega;E)} := (\mathbb{E}(\|X\|_E^p))^{1/p}, \ 1 \leq p < \infty . \tag{2.2}$$

2.1 Modeling of random inputs.

Equipped with the above notation, we will model inputs such as initial data, fluxes, coefficients and sources in (1.1) as random fields. To be more specific, we first model uncertain initial data by assuming $(\Omega, \mathcal{F}, \mathbb{P})$ as the underlying probability space and realizing the uncertain initial data as a random field $\mathbf{U}_0$, i.e. a $L^1(\mathbb{R}^d)$-valued random variable which is a $L^1(\mathbb{R}^d)$ measurable map

$$\mathbf{U}_0 : (\Omega, \mathcal{F}) \longmapsto ((L^1(\mathbb{R}^d))^N, \ (\mathcal{B}(L^1(\mathbb{R}^d)))^N) . \tag{2.3}$$

Similarly, the source term $\mathbf{S}$ and coefficient $\mathbf{c}$ can be modeled as random fields taking for instance values in L^p spaces. It might be essential to also assume further regularity on the coefficient, for instance

$$\mathbf{c}(\cdot, \omega) \in L^\infty(\mathbb{R}^d \times \mathbb{R}_+) \cap BV(\mathbb{R}^d \times \mathbb{R}_+) \quad \mathbb{P}\text{-a.s.}, \tag{2.4}$$

which is to say that

$$\mathbb{P}(\{\omega \in \Omega : \mathbf{c}(\cdot, \omega) \in (L^\infty \cap BV)(\mathbb{R}^d \times \mathbb{R}_+)\}) = 1 . \tag{2.5}$$

Similarly, the flux function $\mathbf{F}$ can also be modeled as a random field, for instance taking values in the space of continuously differentiable functions [68].

2.1.1 Concerte representations.

In practice, one has to realize the random fields for initial data, fluxes, sources, coefficients etc by representing them in a concrete manner. A very common representation of random fields in engineering practice is to realize them in terms of a finite set of parameters. For instance, consider a classic one-dimensional Sod shock tube [61], which consists of two constant states (a left and a right state), with jumps in density and pressure and initial zero velocity. The initial data is completely described by 5 parameters, namely the initial left (and right) densities and pressures and the location of the initial jump. So, one can argue that the initial jump location as well as amplitudes of the initial jumps are uncertain by specifying initial probability distributions in terms of 5 (or less) parameters.

A more rigorous way of defining initial parametrizations is in terms of a Karhunen-Loeve expansion. To introduce this concept, we consider a simple example of a centered random field $u : \Omega \mapsto L^2(D)$, for some domain $D \subset \mathbb{R}^d$ and assume that $\mathbb{E}(u) = 0$. Then, the covariance function of this random field is defined as

$$C_u \in L^2(D \otimes D) : \quad C_u(x, y) = \mathbb{E}(u(x, \omega)u(y, \omega)). \tag{2.6}$$

The corresponding covariance operator is defined as,

$$K_C : L^2(D) \mapsto L^2(D) : \quad K_C[g](x) := \int_D C_u(x, y)g(y)dy. \tag{2.7}$$

One can readily show that K_C is a compact operator and we denote its eigenvalues and eigenfunctions as λ_k and u_k respectively i.e,

$$K_C[u_k] = \lambda_k u_k.$$

Consequently, one can rewrite the underlying random field u as

$$u(x, \omega) = \sum_{k=1}^{\infty} Z_k(\omega)u_k(x). \tag{2.8}$$

Furthermore, one can also show that the random variables Z_k are uncorrelated as

$$\mathbb{E}(Z_j Z_k) = \lambda_k \delta_{jk}$$

Hence, the Karhunen-Loeve expansion is a *biorthogonal* expansion of the underlying random field. By including a non-zero mean and rescaling, one can write any random field in terms of its Karhunen-Loeve expansion as

$$u = \bar{u} + \sum_{k=1}^{\infty} \sqrt{\lambda_k} Z_k u_k, \tag{2.9}$$

with $\bar{u}$ being the mean value of the random field. The Karhunen-Loeve expansion is a hierarchical expansion and one can truncate (2.9) with finitely many terms M. The size of M is determined by the rate of decay of the eigenvalues λ_k, which in turn, depends on the range of correlations of the underlying random field. Thus, the final statistical input is described by a finite number of independent random parameters Z_k. The above description is merely heuristic and more rigorous presentations can be found out, for instance in [68], for the specific case of Karhunen-Loeve expansions of random flux functions.

Modifications of Karhunen-Loeve expansions include spectral representations such as log-normal rock permeabilities, described in [67] for the acoustic wave equation of siesmic imaging and in [23] for permeabilities in flows in porous media. Similarly, other hierarchical representations, such as those based on wavelets can be used to represented bottom topographies of shallow water flows, for instance in [65].

2.2 Random entropy solutions.

Given the above random field representation of uncertain inputs, one can model the resulting uncertain solutions of (1.1) by random fields and formally require them to satisfy the following random version of (1.1):

$$\begin{aligned} \partial_t \mathbf{U}(x,t,\omega) + \nabla_x \cdot \mathbf{F}(\mathbf{c}(x,t,\omega), \mathbf{U}(x,t,\omega), \omega) &= \mathbf{S}(x,t,\mathbf{U},\omega), \\ \mathbf{U}(x,0,\omega) &= \mathbf{U}_0(x,\omega). \end{aligned} \tag{2.10}$$

Here, $\mathbf{U}_0, \mathbf{S}, \mathbf{c}, \mathbf{F}$ are all random fields, taking values in appropriate function spaces, for instance, $\mathbf{U}_0$ is defined in (2.3).

Consequently, we define the random entropy solution $\mathbf{U}$ of (2.10) as follows,

Definition 2.1. A random field $\mathbf{U} : \Omega \mapsto \left(L^1_{\text{loc}}(\mathbb{R}^d \times \mathbb{R}_+)\right)^N$, is a *random entropy solution* of the random balance law (2.10) with random initial data, flux, source and coefficient, if it satisfies the following conditions:

(i.) Weak solution: for $\mathbb{P}$-a.e $\omega \in \Omega$, $\mathbf{U}(\cdot,\cdot;\omega)$ satisfies the following integral identity, for all test functions $\varphi \in C^1_0(\mathbb{R}^d \times \mathbb{R}_+)$:

$$\begin{aligned} &\int_{R_+} \int_{R^d} \left(\mathbf{U}(\omega)\varphi_t + \sum_{j=1}^{d} \mathbf{F}^j(\mathbf{c}^j(\omega), \mathbf{U}(\omega), \omega)\varphi_{x_j} + \mathbf{S}(x,t,\mathbf{U}(\omega),\omega)\varphi \right) dxdt \\ &+ \int_{R^d} \mathbf{U}_0(x,\omega)\varphi(x,0)dx = 0. \end{aligned} \tag{2.11}$$

(ii.) Entropy condition. $\mathbf{U}(\cdot,\cdot,\omega)$ satisfies the underlying entropy condition for (1.1) for almost every $\omega \in \Omega$.

■

The above notion of random entropy solutions was first proposed in [63]. It is a pointwise (a.e) notion that requires that the balance law be satisfied for almost every realization in the probability space Ω. Rigorous existence and uniqueness results for random entropy solutions for scalar conservation laws, with random initial data, were obtained in [63]. Well-posedness results for scalar conservation laws with random fluxes were obtained recently in [68]. A corresponding notion of random weak solutions for multi-dimensional linear symmetrizable hyperbolic systems, with random initial data and random coefficients, were obtained in [37, 67]. In all these cases, the random entropy solutions were shown to be of the form:

$$\mathbf{U}(x,t,\omega) = \mathcal{S}_t(\mathbf{U}_0(x,\omega)), \tag{2.12}$$

where $\mathcal{S}_t : L^p(D) \mapsto L^p(D)$ is the data to solution operator of the underlying deterministic problem. Here, $p = 1$ for scalar conservation laws and $p = 2$ for linear symmetrizable systems. Consequently, the above described notion of random entropy solution only makes sense when the underlying deterministic problem is well-posed. In the following sections, we will assume that random entropy solutions are well-posed and discuss efficient algorithms for approximating them.

3 Stochastic Galerkin method for UQ

Our aim is to design efficient numerical approximations of random entropy solutions of the system of random balance laws (2.10). For simplicity of notation and ease of exposition, we assume that the random balance law is a conservation law i.e, $\mathbf{S} \equiv 0$ in (2.10). We also assume that the only source of uncertainty in (2.10) is in the initial data $\mathbf{U}_0$. This can be realized by setting the coeffiicent $\mathbf{c} = 1$ (for almost every $\omega \in \Omega$) and taking a deterministic flux function $\mathbf{F}$ in (2.10). For further notational simplicity, we consider the random system of conservation laws in *one space dimension*. The extension to several space dimensions is straightforward though notationally cumbersome. Hence, we will consider the following random conservation law,

$$\begin{aligned} \partial_t \mathbf{U}(x,t,\omega) + \partial_x \mathbf{F}(\mathbf{U}(x,t,\omega)) = 0, \quad \forall (x,t) \in D \times \mathbb{R}_+, \ \mathbb{P}\ a.e\ \omega \in \Omega \\ \mathbf{U}(x,0,\omega) = \mathbf{U}_0(x,\omega), \quad \forall x \in D, \ \mathbb{P}\ a.e\ \omega \in \Omega. \end{aligned} \tag{3.1}$$

Here $D = (x_L, x_R) \subset \mathbb{R}$ is the computational domain.

For both the stochastic Galerkin methods described here and the stochastic collocation methods, presented in the following section, we will assume that the uncertainty in the initial data (and consequently in the random entropy solution of (3.1)) satisfies the following *finite dimensional noise* assumption,

Assumption 3.1. *(Finite dimensional noise). The initial data in* (3.1) *has the form,*

$$\mathbf{U}_0(x,\omega) = \mathbf{U}_0(x, Y_1(\omega), Y_2(\omega), \ldots, Y_P(\omega)), \quad \text{on} \quad D \times \Omega. \tag{3.2}$$

Here, P is a (possibly large) constant and Y_p's for $1 \leqslant p \leqslant P$ are real valued random variables.

We denote $\Gamma_p = Y_p(\Omega)$ as the image of Ω under Y_p and denote $\Gamma = \prod_{p=1}^{P} \Gamma_p$. Furthermore, we assume that the random variables $\{Y_1, \ldots, Y_P\}$ have a joint probability density function denoted by $\rho : \Gamma \mapsto \mathbb{R}_+$ with $\rho \in L^\infty(\Gamma)$. For simplicity, we assume that ρ can be factorized as $\rho(Y_1, \ldots, Y_P) = \prod_{p=1}^{P} \rho_p(Y_p)$. The reader can observe that this assumption is valid for any (finite-dimensional) parametric representation of uncertainty, as described in section 2, for instance, with a truncation of the Karhunen-Loeve representation of uncertain initial data.

3.1 Generalized Polynomial Chaos (gPC)

The key step in numerically approximating the conservation law (3.1) lies in discretizing the probability space Ω. Following [45], any random field $h \in L^2(\Omega, L^2(\mathbb{R} \times \mathbb{R}_+))$ can be written as,

$$\mathbf{h} = \sum_{k=0}^{\infty} \mathbf{h}^k(x,t) \varphi^k(\mathbf{y}(\omega)). \tag{3.3}$$

Here, $\mathbf{y} = \{y_1, y_2, \ldots, \}$ are a set of independent, identically distributed (i.i.d) random variables with zero mean and φ^k are a set of orthogonal polynomials with respect to the underlying measure ρ. Furthermore, the coefficients $\mathbf{h}^k$ in (3.3) are purely deterministic functions, independent of ω. The orthogonal polynomials φ are dependent on the measure ρ and consequently on its probability density function $\rho(\mathbf{y})$. As examples, one can choose Legendre polynomials for uniform distributions and Hermite polynomials if the underlying probability distribution function is Gaussian.

In order to construct a numerical method, we will use the finite noise assumption above and find P such that $\mathbf{y} = \{y_1, y_2, \ldots, y_P\}$. Hence, the expansion provides a parametrization of the probability space Ω in terms of the coordinates $\Gamma = \prod_{i=1}^{P} \Gamma_i$ with $y_i \in \Gamma_i$ for all $1 \leqslant i \leqslant P$. Furthermore, we have to truncate the infinite series in (3.3) by choosing a L such that,

$$\mathbf{h}_P^L = \sum_{l=0}^{L} \mathbf{h}^l(x,t) \varphi^l(\mathbf{y}). \tag{3.4}$$

The convergence of $\mathbf{h}_P^L$ to $\mathbf{h}$ as $L, P \to \infty$ is guaranteed by the Cameron-Martin theorem [59]. For convenience, we tag the two indices L and P in (3.4) into a single index, still denoted by L. The orthogonal polynomials φ are now constructed as tensor products of one-dimensional orthogonal polynomials, i.e,

$$\varphi^k(\mathbf{y}) = \otimes_i \varphi^{k_i}(y_i), \tag{3.5}$$

with the maximum degree of k_i's being set to M (depending on accuracy requirements). With the above structure, the total number of terms in the expansion is

$$L = \frac{(M+P)!}{M!P!} - 1.$$

We will employ the truncated generalized Polynomial chaos (gPC) expansion in-order to design robust numerical schemes for approximating (3.1).

3.2 Standard stochastic Galerkin (sG) method.

We follow a large number of recent papers, such as [17, 47, 24, 25, 32, 33, 82] and references therein, and aim to approximate the random entropy solution $\mathbf{U}$ of (3.1) by its truncated gPC expansion (3.4) realized as,

$$\mathbf{U} \approx \mathbf{U}^L = \sum_{l=0}^{L} \mathbf{U}^l(x,t)\varphi^k(\mathbf{y}). \tag{3.6}$$

Here, φ^k are the ρ-orthogonal polynomials described in the previous sub-section. The expansion (3.6) is valid as long as the solution $\mathbf{U}$ of (3.1) has bounded second moments.

The moments $\mathbf{U}^l$ in (3.6) are computed by using the Galerkin projection in the random space Γ i.e,

$$\mathbf{U}^l(x,t) = \int_\Gamma \mathbf{U}(x,t)\varphi^l(\mathbf{y})\rho(\mathbf{y})d\mathbf{y}, \tag{3.7}$$

with $\mathbf{U}^L$ being denoted as $\mathbf{U}$ (for notational simplicity) and $\rho(\mathbf{y})$ being the probability density function of the underlying measure ρ. In-order to compute the moments, we perform a Galerkin approximation of (3.1) and a projection to the truncated expansion to obtain,

$$\frac{\partial}{\partial t}\left(\sum_{l=0}^{L}\int_\Gamma U^l\varphi^l\varphi^j\rho(\mathbf{y})d\mathbf{y}\right) + \frac{\partial}{\partial x}\left(\int_\Gamma \mathbf{F}\left(\sum_{l=0}^{L}\mathbf{U}^l\varphi^l\right)\varphi^j\rho(\mathbf{y})d\mathbf{y}\right) = 0, \quad \forall\, 0 \leqslant j \leqslant L. \tag{3.8}$$

By using orthogonality of the polynomials φ, (3.8) reduces to the following system of equations,

$$\begin{aligned} &\partial_t \mathbf{U}^j + \partial_x(\mathbf{F}^j(\mathbf{U}^1,\ldots,\mathbf{U}^j,\ldots,\mathbf{U}^L) = 0, \quad \forall\, 0 \leqslant j \leqslant L,\\ &\mathbf{F}^j = \left(\int_\Gamma \mathbf{F}\left(\sum_{l=0}^{L}\mathbf{U}^l\varphi^l\right)\varphi^j\rho(\mathbf{y})d\mathbf{y}\right), \quad \forall\, 0 \leqslant j \leqslant L. \end{aligned} \tag{3.9}$$

Thus the spectral Galerkin projection of (3.1) leads to a $LN \times LN$ (N being the phase space dimension) system of equations. Note that the variables $\mathbf{U}^j$ are coupled through non-linear fluxes. The uncertain initial data in (3.1) can similarly be expanded and its moments calculated. Uncertainty quantification routines for (3.1) involve suitable discretizations of the system (3.9), for instance using standard finite difference, finite volume, discontinuous Galerkin finite element schemes or any type of method using continuous finite element. In particular, is straigthtforward to calculate the statistical moments of the random field $\mathbf{U}$ from the weights $\mathbf{U}^l$. For example, the mean and variance of $\mathbf{U}$ can be computed as,

$$\begin{aligned} \mathbb{E}(\mathbf{U}) &= \mathbf{U}^0,\\ \sigma^2 = \mathbb{E}((\mathbf{U}-\mathbf{U}^0)^2) &= \sum_{l=1}^{L}(\mathbf{U}^l)^2. \end{aligned} \tag{3.10}$$

The gPC system (3.9) is an $LN \times LN$ system of conservation laws. In particular, even for a scalar conservation law ($N = 1$), the gPC system is an $L \times L$ system. The system size L can be very large if the random initial data is represented by a large number of random parameters, such as in a slowly decaying Karhunen-Loeve expansion. Furthermore, the calculation of the gPC coefficients $\mathbf{U}^j$ and the fluxes $\mathbf{F}^j$ in (3.9) requires integrating over the random space Γ that is P-dimensional. Using full tensor product quadrature for computing such integrals is very expensive and sparse grids have been used [32] and references therein. Still, the computational cost can be formidable. However, a more fundamental difficulty arises when analyzing system (3.9). It is unclear if this system is even *hyperbolic*. Since, the entire machinery of analyzing and discretizing conservation laws assumes hyperbolicity, it is unclear even if the system (3.9) makes any mathematical sense.

3.3 gPC expansions in the entropy variables.

The system (3.9) results from expanding the conserved variables $\mathbf{U}$ of (3.1) in terms of a gPC expansion. We aim to find a *different* expansion such that the resulting truncated system possesses hyperbolicity. Such an expansion was proposed in [26], in turn inspired by analogous problems in kinetic theory of gases as presented in [30].

The fundamental assumption in this approach is that the underlying conservation law possesses a convex *entropy function* S and an entropy flux function Q. Then, the idea is to expand in terms of the entropy variables $\mathbf{V} = \partial_{\mathbf{U}}(S(\mathbf{U}))$. The convexity of the entropy function S implies that there is a one to one mapping,

$$\mathbf{U}(\mathbf{V}) : \mathbb{R}^N \mapsto \mathbb{R}^N, \tag{3.11}$$

such that $\mathbf{U}(\mathbf{V})$ is invertible for all $\mathbf{V} \in \mathbb{R}^N$. Hence, (3.1) can be rewritten in terms of entropy variables as,

$$\partial_t \mathbf{U}(\mathbf{V}(x,t,\mathbf{y})) + \partial_x \mathbf{F}(\mathbf{V}(x,t,\mathbf{y})) = 0. \tag{3.12}$$

Here, $\mathbf{y} \in \Gamma$ is a parametrization of the random space Ω and $\mathbf{F}(\mathbf{V}) = \mathbf{F}(\mathbf{U}(\mathbf{V}))$ results from expressing the flux in terms of entropy variables.

Following [30, 26], one expands the entropy variables $\mathbf{V}$ in terms of a truncated gPC expansion,

$$\mathbf{V} \approx \mathbf{V}^L = \sum_{l=0}^{L} \mathbf{V}^l(x,t)\varphi^l(y). \tag{3.13}$$

Here, the orthogonal polynomials φ are defined by (3.5) and $\mathbf{V}^l$ are the corresponding (independent of $\mathbf{y}$) weights. The set-up is exactly the same as the previous sub-section. We expand all the terms in (3.12) in terms of the truncated expansion (3.13) and mutliply with all orthogonal polynomials φ to obtain the following system:

$$\begin{aligned}
\frac{\partial}{\partial t}\mathcal{U}^j + \frac{\partial}{\partial x}\mathcal{F}^j &= 0, \quad \forall\, 0 \leqslant j \leqslant L, \\
\mathcal{U}^j = \mathcal{U}^j(\mathbf{V}^1,\ldots,\mathbf{V}^j,\ldots,\mathbf{V}^L) &= \int_\Gamma \mathbf{U}\left(\sum_{l=0}^{L}\mathbf{V}^l\varphi^l\right)\varphi^j\rho(\mathbf{y})dy, \\
\mathcal{F}^j = \mathcal{F}^j(\mathbf{V}^1,\ldots,\mathbf{V}^j,\ldots,\mathbf{V}^L) &= \int_\Gamma \mathbf{F}\left(\mathbf{U}\left(\sum_{l=0}^{L}\mathbf{V}^l\varphi^l\right)\right)\varphi^j\rho(\mathbf{y})dy.
\end{aligned} \tag{3.14}$$

Here, $\mathbf{U}(\mathbf{V})$ is the function transforming entropy variables into conservative variables. The above system (3.14) is a $LN \times LN$ system of non-linear conservation laws. The coupling between the variables is now through the non-linear flux as well as the non-linear *temporal* flux as the mass matrix of the underlying Galerkin approximation is no longer diagonal. The aim is to approximate (3.14), in order to construct approximations of (3.12).

One can prove that the system (3.14) satisfies an entropy inequality of the form,

$$\mathcal{S}_t + \mathcal{Q}_x \leqslant 0. \tag{3.15}$$

Here, the entropy function and entropy flux are defined by,

$$\begin{aligned}
\mathcal{S}(x,t) &= \int_\Gamma S\left(\sum_{l=0}^{L}\mathbf{V}^l\varphi^l\right)\rho(\mathbf{y})d\mathbf{y}, \\
\mathcal{Q}(x,t) &= \int_\Gamma Q\left(\sum_{l=0}^{L}\mathbf{V}^l\varphi^l\right)\rho(\mathbf{y})d\mathbf{y}.
\end{aligned} \tag{3.16}$$

Furthermore, the entropy function $\mathcal{S}$ is convex. Hence, by the Godunov-Mock theorem, the system is hyperbolic. Consequently, the system (3.14) inherits the entropy framework from the underlying conservation law. Once the hyperbolicity is shown, (3.14) can be discretized using the standard finite difference, finite volume or finite element methodology for hyperbolic systems and the resulting statistical quantities of interest, computed in terms of the gPC coefficients $\mathbf{V}^l$. In addition to the difficulties of possibly large system size, the discretization of (3.14) has to confront the issue of inverting the non-diagonal mass matrix $\mathbf{U}(\mathbf{V})$ at each time step. This can be done using a

Newton method. It is straightforward, though notationally cumbersome, to derive the analogue of (3.14) in several space dimensions.

However, given the already formidable computational cost of solving a high-dimensional system with a large number of parameters, there have been many recent attempts to find gPC type expansions that guarantee hyperbolicity of the resulting truncated system without resorting to the expansion in entropy variables and the consequent retrieval of the entropy variables by solving nonlinear systems at each time step. One such attempt is in [4, 3] and references therein, where the authors present a novel splitting of the underlying system and expand the split systems in a gPC basis in order to ensure that the resulting gPC system is hyperbolic. Such splittings have been obtained for the one-dimensional shallow water and Euler equations.

Summing up, the stochastic Galerkin method provides a robust UQ framework, particularly when the gPC expansion is in the entropy variables. The statistical moments and in fact, the entire solution random field, can be computed. However, the computational cost is very high, particularly when the random inputs have a large number of parameters. The lack of regularity, particularly with respect to uncertain parameters, inhibits the use of compression techniques, such as those proposed in [5] for elliptic PDEs, that can lead to amelioration of the curse of dimensionality. Moreover, the stochastic Galerkin method is *intrusive*. New code has to be written in order to discretize (3.9) or (3.14). This prevents widespread use of this method as reusing existing code would be highly desirable.

4 Stochastic collocation methods.

One class of *non-intrusive* methods for uncertainty quantification are the so-called stochastic collocation methods, [18, 81] and references therein. In the present context, we describe stochastic collocation methods to approximate the one-dimensional conservation law (3.1) with random initial data. The extension to several space dimensions and uncertain fluxes, coefficients, sources, etc, is straightforward but involves complicated notation. To begin with, we use the finite noise assumption and transform the random conservation law (3.1) to the following *parametric conservation law*,

$$\begin{aligned} \partial_t \mathbf{U}(x,t,\mathbf{y}) + \partial_x \mathbf{F}(\mathbf{U}(x,t,\mathbf{y})) = 0, \quad (x,t,\mathbf{y}) \in (\mathbb{R},\mathbb{R}_+,\Gamma), \\ \mathbf{U}(x,0,\mathbf{y}) = \mathbf{U}_0(x,\mathbf{y}), \quad (x,\mathbf{y}) \in (\mathbb{R},\Gamma). \end{aligned} \tag{4.1}$$

Here, Γ is the P-dimensional parametric representation of the probability space Ω, described in section 3.

4.1 Standard stochastic collocation method

The standard collocation method (see [18, 81] and references therein) for discretizing the random space Γ consists of seeking approximations of (4.1) that lie in the function space $L^1(\mathbb{R}\times\mathbb{R}_+)\times\mathcal{P}_l(\Gamma)$ where $\mathcal{P}_l(\Gamma)\subset L^2_\rho(\Gamma)$ is the span of tensor product polynomials of degree at most $l=(l_1,l_2,\ldots,l_P)$; i.e, $\mathcal{P}_l(\Gamma)=\otimes_{n=1}^P\mathcal{P}_{l_n}(\Gamma_n)$ where

$$\mathcal{P}_{l_n} = \text{span}(y_n^m,\ m=0,1,\ldots,l_n), \quad n=1,\ldots,P. \tag{4.2}$$

Sparse tensor products can also be used in representing $\mathcal{P}_p$.

The next step consists of selecting *collocation points* in the random space Γ by choosing zeros of polynomials, orthogonal to the underlying probability density function $\rho(\mathbf{y})$. For each parametric dimension $p=1,\ldots,P$, we denote $y_{k_p}^p$, $1\leqslant k_p\leqslant n_p+1$ be the (n_p+1) roots of the orthogonal polynomial q_{n_p+1} with respect to the weight ρ_p.

Next, at each collocation point on the (sparse) tensor product grid, we can discretize the parametric conservation law (4.1) by any standard method. Once, the solution at each of the collocation points is obtained, statistical quantities of interest like the mean and the variance can be obtained by using suitable quadrature rules. The above procedure is very simple to implement as any code for the underlying deterministic problem can be employed at the appropriate collocation point and the statistics of interest can be readily computed. However, the key principle underlying the convergence of a collocation procedure in the random space is appropriate regularity of the solution in the random space, required in-order to ensure convergence of global approximation polynomials like those considered above. Such a regularity is lacking, in general, for random conservation laws. Consequently, a naive application of the stochastic collocation method results in high frequency spurious oscillations such as those reported in [72] and references therein. Thus, the standard stochastic collocation method is not suitable for approximating random conservation (balance) laws.

4.2 Stochastic finite volume methods.

Given the problems with stochastic collocation methods in discretizing random conservation laws, an alternative that takes into account discontinuities of the random entropy solution with respect to the uncertain parameters $\mathbf{y}$ is the so-called *stochastic finite volume method*. Variants of this method have been proposed in [49], then [53, 73, 72, 68, 31] and references therein.

Here we follow the presentation of [49, 53, 54]. For simplicity, we consider the one-dimensional random (parametric) conservation law (4.1) and the finite-dimensional noise assumption (3.1). Recall that the probability space Ω is represented by the parameter space $\Gamma \subset \mathbb{R}^P$. Furthermore, the underlying measure on Γ is ρ (we do not need assume that ρ is a tensor product measure in this section). We abuse notation slightly to denote as,

$$\mathbb{E}(\Psi(\mathbf{y})) = \int_\Gamma \Psi(\mathbf{y}) d\rho(\mathbf{y}),$$

the *expectation* of a measurable function Ψ with respect to the measure ρ.

We consider a spatial discretisation for (4.1) with node points $x_i = i\Delta x$ where i belongs to some subset of $\mathbb{Z}$, a time step $\Delta t > 0$ and set $t_n = n\Delta t$, $n \in \mathbb{N}$. The control volumes are, as usual, the intervals $C_i = [x_{i-1/2}, x_{i+1/2}]$ with $x_{i+1/2} = \frac{x_i + x_{i+1}}{2}$. We have uniform, $|C_i| = \Delta x$, here, for simplicity only. We start from a finite volume scheme, and again for the simplicity of exposition, we only consider a first order in time and space scheme. The generalization to more accurate scheme is obvious, as well as to multi-dimensional problems, see [69] for an example using DG method or [54] for an example using Residual Distribution methods.

Thus we define the *deterministic scheme* as

$$\mathbf{U}_i^{n+1} = \mathbf{U}_i^n - \frac{\Delta t}{\Delta x}\left(\hat{\mathbf{F}}(\mathbf{U}_i^n, \mathbf{U}_{i+1}^n) - \hat{\mathbf{F}}(\mathbf{U}_{i-1}^n, \mathbf{U}_i^n)\right) \tag{4.3}$$

with $\mathbf{U}_i^0$ being an approximation of $\int_{C_i} \mathbf{U}_0(x)dx/|C_i|$ and $\hat{\mathbf{F}}$ a consistent approximation of the underlying continuous flux $\mathbf{F}$.

When $\mathbf{U}_0$ or the flux $\mathbf{F}$ are uncertain, we perform the following procedure. First the set $\Gamma \subset \mathbb{R}^P$ is subdivided into non overlapping subsets Γ_j, $j = 1, \ldots, n_p$ and the variables are represented by their conditional expectations in the Ω_j subsets. More precisely, our set of unknowns is

$$\mathbf{U}_{i,j}^n \approx \frac{\mathbb{E}\left(\int_{C_i} U(x, t_n, \mathbf{y}) \; | \mathbf{y} \in \Gamma_j\right)}{|C_i| \; \rho(\Gamma_j)}.$$

which evolves in time as

$$\mathbf{U}_{i,j}^{n+1} = \mathbf{U}_{i,j}^n - \frac{\Delta t}{\Delta x}\left(\mathbb{E}(\hat{\mathbf{F}}(\mathbf{U}_i^n, \mathbf{U}_{i+1}^n) \; | \Gamma_j) - \mathbb{E}(\hat{\mathbf{F}}(\mathbf{U}_{i-1}^n, \mathbf{U}_i^n) \; | \Gamma_j)\right).$$

The scheme is fully defined provided the "flux" $\mathbb{E}(\hat{\mathbf{F}}(\mathbf{U}_l^n, \mathbf{U}_{l+1}^n) \; | \Gamma_k)$ can be evaluated for any l and k.

This is the exactly the same issue that arises in solving the reconstruction problem for finite volume methods, with the additional constraint that the underlying measure is $d\rho$ instead of the standard Lebesgue measure. We are given a decomposition of Γ by non overlapping subsets Γ_i, $i = 1, n_p$ of strictly positive measure:

$$\Gamma = \cup_{j=1}^N \Gamma_j, \qquad \rho(\Gamma_j) > 0.$$

We are given the conditional expectations, $\mathbb{E}(\mathbf{y}|\Gamma_j)$. Can we estimate for a given measurable function f, $\mathbb{E}(f(\mathbf{y}))$? Recall that $\mathbf{y} = (y_1, \ldots, y_P)$, we do the following, for each Γ_i, we wish to evaluate a multivariate polynomial $P_i \in P^n(\Gamma_1)$ of degree n such that

$$E(\mathbf{y}|\Gamma_j) = \frac{\int_{\mathbb{R}^P} 1_{\Gamma_j}(\mathbf{y}) P(\mathbf{y}) \; d\rho}{\rho(\Gamma_j)} \qquad \text{for } j \in \mathcal{S}_i. \tag{4.4}$$

Here, $\mathcal{S}_i$ is a stencil associated to Γ_i. This problem is reminiscent of what is done in finite volume schemes to compute a polynomial reconstruction in order to increase the accuracy of the flux evaluation thanks to the MUSCL extrapolation. Among the many references that have dealt with this problem, with the Lebesgue measure

$dx_1 \otimes dx_2 \ldots \otimes dx_n$, one may quote [6] and for general meshes [71, 48]. A systematic method for computing the solution of problem (4.4) is given in [57].

Assume that the stencil $\mathcal{S}_i$ is defined, the technical condition that ensures a unique solution to problem (4.4) is that the Vandermonde–like determinant (given here for one parametric variable for the sake of simplicity)

$$\Delta_i = \det\left(\mathbb{E}(y^l|\Gamma_j)\right)_{0\leqslant l\leqslant n,\, j\in\mathcal{S}_i}. \tag{4.5}$$

is non zero. In the case of several random variable, the exponent l in (4.5) is replaced by a multi–index.

Once the solution of (4.4) is known, we can estimate

$$\sum_{j=1}^{N}\int_{\Gamma_j} f(P(\mathbf{y}))\; d\rho(\mathbf{y}).$$

The following approximation results hold : if $f \in C^p(\mathbb{R})$ with $p \geqslant n$ then

$$\left|\mathbb{E}(f(\mathbf{y})) - \sum_{j=1}^{N}\int_{\Gamma_j} f(P(\mathbf{y}))\; d\rho(y)\right| \leqslant C(\mathcal{S}) \max_j\, [\rho(\Gamma_j)^{p+1}]$$

for a set of regular stencils.The proof is a straightforward generalization of the approximation results contained in [46].

Centered, ENO and WENO-like such reconstructions, with and without tensorisation, have been considered in [54, 69], in particular to handle possible discontinuities in the pdf and the solution. From a technical point of view, any kind of pdf can be handled and the evaluation of the conditional expectations are performed with *fixed* Gaussian-like quadrature rules: again see [54, 69] for details.

Summarizing, the stochastic finite volume method provides a possible UQ framework for random conservation (balance) laws. It is non-intrusive, simple to implement and able to approximate discontinuities in the random parametric space. However, the lack of regularity of the random solutions on the uncertain parameters precludes gains in complexity by employing sparse grids or sparse tensor products. Consequently, the curse of dimensionality only allows this method to be viable for a small to moderate number of sources of uncertainty. A notable exception is provided in [68] where the authors use special properties of a scalar conservation law with random flux functions, to design an adaptive hierarchical grid in the parameter space. With the resulting method, the authors were able to overcome the curse of dimensionality due to the hierarchical dependence of the solution on parameters. However, extensions of this approach to systems of conservation laws is unclear. In [55] the authors were partialy successful in facing the curse of dimensionality via a multi-resolution method using Harten's [29] framework, the price to pay was an added complexity of the algorithm. This method was used in [56] for solving multiphase problems, and in [41] some geophysical problems involving tsunamis.

5 Monte Carlo and Multi-level Monte Carlo methods.

Both the intrusive stochastic Galerkin method and the non-intrusive stochastic collocation finite volume method, described above, suffer from the curse of dimensionality. An alternative paradigm that is robust with respect to handling a large number of sources of uncertainty is that of statistical sampling methods or Monte Carlo methods.

5.1 Monte Carlo method

Our aim is to approximate the random balance law (2.10). The spatio-temporal discretization can be performed by any standard Finite Volume or DG scheme, for instance (1.5). The probability space will be discretized using a Monte Carlo (MC) algorithm consisting of the following three steps:

1. **Sample:** We draw M independent identically distributed (i.i.d.) initial data, flux, source term and coefficient samples $\{\mathbf{U}_0^l, \mathbf{F}_j^l, \mathbf{S}^l, \mathbf{c}^l\}$ with $j = 1, \cdots, d$ and $l = 1, 2, \ldots, M$ from the random fields $\{\mathbf{U}_0, \mathbf{F}_j, \mathbf{S}, \mathbf{c}\}$ and approximate these by piecewise constant cell averages.

2. **Solve:** For each realization $\{\mathbf{U}_0^l, \mathbf{F}_j^l, \mathbf{S}^l, \mathbf{c}^l\}$, the underlying balance law (2.10) is solved numerically by the finite volume method (1.5) (or any suitable finite difference or finite element methods). We denote the FVM solutions by $\mathbf{U}_{\mathcal{T}}^{l,n}$, i.e. by cell averages $\{\mathbf{U}_C^{l,n} : C \in \mathcal{T}\}$ at the time level t^n,

$$\mathbf{U}_{\mathcal{T}}^{l,n}(x) = \mathbf{U}_C^{l,n}, \quad \forall x \in C,\ C \in \mathcal{T},\ l = 1, ..., M\ .$$

3. **Estimate Statistics:** We estimate the expectation of the random solution field with the sample mean (sample average) of the approximate solution:

$$E_M[\mathbf{U}_{\mathcal{T}}^n] := \frac{1}{M}\sum_{l=1}^{M} \mathbf{U}_{\mathcal{T}}^{l,n}. \tag{5.1}$$

   Higher statistical moments can be approximated analogously under suitable statistical regularity of the underlying random entropy solutions [63].

The above algorithm is, at first sight, straightforward to implement. We remark that step 1 requires a (pseudo) random number generator. Here, care must be exercised in ensuring good statistical properties in massively parallel implementations (see [38, 66, 35] for details). In step 2, any standard (high-order) finite volume or DG scheme can be used. Hence, existing ("legacy") code for FVM (or DG) can be (re) used and there is no need to rewrite FVM (or DG) code. Furthermore, the only (data) interaction between different samples is in step 3 when ensemble averages are computed. Thus, the MC-FVM is non-intrusive as well as easily parallelizable.

5.1.1 Error and complexity analysis.

In order to prove a rigorous error estimate for the Monte Carlo finite volume approximation of the random entropy solution of (2.10), one needs to assume that the underlying spatio-temporal discretization, for instance the finite volume approximation (1.5) satisfies the following error estimate,

$$\|\mathbf{U}(\cdot, T) - \mathbf{U}_{\mathcal{T}}(\cdot, T)\|_{L^1(D)} \leqslant C(D, T)\Delta x^s. \tag{5.2}$$

Here, we denote $\mathbf{U}_{\mathcal{T}}$ to be the piecewise constant solution obtained by the finite volume scheme (1.5) and $\Delta x = \Delta x_{\mathcal{T}}$ is the (spatial) mesh parameter, which is also related to the time step through the CFL number. Such an error estimate holds for a standard monotone finite volume scheme with $s \leqslant 1$ for multi-dimensional scalar conservation laws. However, such a rigorous estimate is not available for systems of conservation laws.

Once we assume an error estimate for the spatio-temporal discretization, one can prove the following error estimate for the Monte Carlo finite volume method (see [68] for the statement and proof of the rigorous result):

$$\|\mathbb{E}[\mathbf{U}(\cdot, t^n)] - E_M[\mathbf{U}_{\mathcal{T}}^n]\|_{L^2(\Omega;L^1(D))} \leq C_{\text{stat}} M^{-\frac{1}{2}} + C_{\text{st}}\Delta x^s, \quad \forall n > 0. \tag{5.3}$$

The constants $C_{\text{stat}}, C_{\text{st}}$ depend only on the second order statistics of the random inputs, the final time T and the spatial domain D.

Note that the error estimate for the mean requires that the random field solution has finite second moments. An analogous error estimate can be derived for higher moments of the solution, provided that the underlying solution has finite higher-order moments. Based on the error analysis of [63, 68], we equilibrate the discretization and the sampling errors in the a-priori estimate (5.3) and choose [64]

$$M = O(\Delta x^{-2s}), \tag{5.4}$$

in-order to equilibrate the statistical error in (5.3) with the spatio-temporal error. With the choice (5.4), it is straightforward to deduce that the asymptotic error vs. (computational) work estimate is then given by

$$\|\mathbb{E}[u(\cdot, t^n)] - E_M[u_{\mathcal{T}}^n]\|_{L^2(\Omega;L^1(D))} \lesssim (\text{Work})^{-s/(d+1+2s)}. \tag{5.5}$$

Here Work refers to the computational work that scales with the number of arithmetic operations (flops). The above error vs. work estimate is considerably more expensive when compared to the underlying finite volume discretization error for the corresponding deterministic problem, which scales as $(\text{Work})^{-s/(d+1)}$ [63].

Hence, the Monte Carlo method is non-intrusive, easy to implement and parallelize and robust to the number of uncertain dimensions (does not suffer from the curse of dimensionality). However, as indicated in (5.5), it is very expensive computationally.

5.2 Multi-level Monte Carlo Finite Volume Method

The low convergence rate (5.5) of the Monte Carlo method motivates the design of Multi-Level Monte Carlo (MLMC) method, first proposed in [62] for numerical quadrature and [42] for solving stochastic differential equations. It was adapted to the PDE context in [2] and to solve random hyperbolic conservation laws in [63, 64, 65, 38, 66, 67, 37, 36, 35, 68] and references therein.

The key idea behind the MLMC method is to simultaneously sample a *hierarchy of discretizations of the PDE with random inputs with a level-dependent number of samples*. In the present setting, this amounts to running a deterministic finite volume solver on a sequence of nested grids in space with correspondingly adapted time step sizes, so as to ensure the validity of a CFL condition uniformly over all space discretizations of the hierarchy [63].

5.2.1 MLMC-FVM algorithm

The Multi-Level Monte-Carlo Finite-Volume (MLMCFVM for short) algorithm consists of the following four steps:

1. **Hierarchy of space-time discretizations:** Consider *nested* triangulations $\{\mathcal{T}_\ell\}_{\ell=0}^{\infty}$ of the spatial domain D with corresponding mesh widths Δx_ℓ that satisfy:

$$\Delta x_\ell = \Delta x(\mathcal{T}_\ell) = \sup\{\mathrm{diam}(K) : \ K \in \mathcal{T}_\ell\} = O(2^{-\ell}\Delta x_0), \tag{5.6}$$

   where Δx_0 is the mesh width for the coarsest resolution and corresponds to the lowest level $\ell = 0$.

2. **Sample:** For each level of resolution ℓ, we draw a *level-dependent number* M_ℓ of independent, identically distributed (i.i.d) samples from the input random fields $\{\mathbf{U}_0, \mathbf{F}_j, \mathbf{S}, \mathbf{c}\}$. Note that these random field inputs are only sampled on $\mathcal{T}_\ell$ in the spatially discrete form, i.e. as realizations of cell-averages on triangulation $\mathcal{T}_\ell$, to yield *vectors* $\{\mathbf{U}_{0,\ell}(\omega), \mathbf{F}_{j,\ell}(\omega), \mathbf{S}_\ell(\omega), \mathbf{c}_\ell(\omega)\}$. on mesh $\mathcal{T}_\ell$. We index the level-dependent number M_ℓ of samples of these vectors by k, i.e. we write

$$\{\mathbf{U}_{0,\ell}^k, \mathbf{F}_\ell^k, \mathbf{S}_\ell^k, \mathbf{c}_\ell^k\}_{k=1}^{M_\ell} = \{\mathbf{U}_{0,\ell}(\omega^k), \mathbf{F}_{j,\ell}(\omega^k), \mathbf{S}_\ell(\omega^k), \mathbf{c}_\ell(\omega_k) : k = 1, ..., M_\ell\} \ .$$

3. **Solve:** For each resolution level $\ell = 0, ..., L$ and for each realization of the random input data $\{\mathbf{U}_{0,\ell}^k, \mathbf{F}_{j,\ell}^k, \mathbf{S}_\ell^k, \mathbf{c}_\ell^k\}$, $k = 1, ..., M_\ell$, the resulting *deterministic balance law* (2.10) (for this particular realization) is solved numerically by the finite Volume method (1.5) (or any other finite difference or finite element method) with mesh width Δx_ℓ. We denote the resulting ensemble of finite volume solutions by $\mathbf{U}_{\mathcal{T}_\ell}^{k,n}$, $k = 1, ..., M_\ell$. These constitute approximate cell averages $\{\mathbf{U}_C^{k,n} : C \in \mathcal{T}_\ell\}$ of the corresponding realization of the random balance law at time level t^n and at spatial resolution level ℓ,

4. **Estimate solution statistics:** Fix some positive integer $L < \infty$, corresponding to the highest level. We estimate the expectation of the random solution field with the following estimator:

$$E^L[\mathbf{U}(\cdot, t^n)] := \sum_{\ell=0}^{L} E_{M_\ell}[\mathbf{U}_{\mathcal{T}_\ell}^n - \mathbf{U}_{\mathcal{T}_{\ell-1}}^n], \tag{5.7}$$

   with E_{M_ℓ} being the MC estimator defined in (5.1) for the level ℓ.

Remark 5.1. Higher statistical moments of the random entropy solution can be approximated analogously (see, e.g., the sparse tensor discretization of [63]). An additional, new issue arises in the efficient numerical computation of *space-time correlation functions* due to the high-dimensionality of such correlation functions. ■

The MLMC-FVM is *non-intrusive* as any standard FVM (or DG) code can be used in step 3. Furthermore, MLMC-FVM is amenable to *efficient parallelization* as data from different grid resolutions and different samples only interacts in step 4.

5.2.2 Error and complexity analysis

One can perform a rigorous error analysis of the MLMC-FVM method under the assumption that the underlying spatio-temporal finite volume discretization (1.5) satisfies the error estimate (5.2). Under this assumption and the added assumption that the initial data was uniformly (in Ω) compactly supported in $\mathbb{R}^d$, it was proved in [68] that the MLMC finite volume method satisfied the error estimate,

$$\|\mathbb{E}[\mathbf{U}(\cdot,t^n)] - E^L[\mathbf{U}(\cdot,t^n)]\|^2_{L^2(\Omega;L^1(D))} \leqslant C_1\Delta x_L^{2s} + C_2\Big\{\sum_{\ell=1}^{L} M_\ell^{-1}\Delta x_\ell^s\Big\} + C_3 M_0^{-1} \tag{5.8}$$

Here, the parameter $s > 0$ refers to the convergence rate of the finite volume scheme for the deterministic problem and $C_{1,2,3}$ are constants depending only on the second moments of the random inputs, the final time T and the spatial domain D.

The error bound (5.8) serves as the basis for a procedure to determine the optimal number M_ℓ of samples at each level such that the resulting computational work is minimized while setting the overall error in (5.8) to behave like Δx_L^{2s}. Using the Lagrange multiplier technique from Giles [43] and references therein, results in, for $0 < s < d+1$,

$$M_\ell \sim \frac{\Delta x_\ell^{\frac{(s+d+1)}{2}}}{\Delta x_L^{2s}} \sum_{j=0}^{L} \Delta x_j^{\frac{(s-(d+1))}{2}} \sim \frac{\Delta x_\ell^{\frac{(s+d+1)}{2}}}{\Delta x_L^{\frac{(3s+d+1)}{2}}} \tag{5.9}$$

Here $A \sim B$ signifies that A and B can be mutually bounded by a (constant) multiple of each other, with this constant being independent of L, ℓ.

As in [68] we use the sample numbers M_ℓ in (5.9) to obtain the following error estimate in terms of computational work,

$$\|\mathbb{E}[u(\cdot,t)] - E^L[u(\cdot,t)]\|_{L^2(\Omega;L^1(D))} \leq C\left(\text{Work}(\{M_\ell\}_{\ell=0}^L;\mathcal{T}_L)\right)^{-s/(d+1+s)} \tag{5.10}$$

The complexity estimate (5.10) shows that the MLMC method is significantly more efficient than the Monte Carlo method (5.5), in terms of computational work that needs to be performed for obtaining the same error. However, to achieve a comparable error in $L^2(\Omega;L^1(D))$, the MLMC method is more expensive than a single deterministic solve.

5.2.3 Efficient implementation and parallelization.

The key issues in the efficient implementation of the MLMC method are to specify the number of levels of resolution and the number of samples at the finest level of resolution. Once these inputs are provided, one can use the formula (5.9) to determine the number of samples at each level of resolution. However, using the a priori determination of samples is perhaps the simplest way of implementing MLMC. More sophisticated algorithms, such as the use of run-up samples [36, 23], a posteriori error estimates [22] or use of continuation MLMC method [44] can be used to determine sharper bounds on the number of levels and the number of samples at each level of resolution.

A key element in the gain of efficiency with MLMC techniques is a scalable implementation on massively parallel HPC (high performance computing) hardware architectures. Unlike Monte Carlo, which is trivially parallelizable, MLMC requires dedicated algorithms to ensure scalability. Both static [38] and dynamic load balancing algorithms [35] have been developed for this purpose and shown to scale to atleast 50000 processors. Hybrid CPU-GPU implementations have also been developed and shown to scale.

5.3 Numerical experiments

We present a few numerical experiments to illustrate the robustness of the stochastic finite volume and MLMC methods.

5.3.1 Compressible Euler equations.

We start with a simple shock tube example that was initially suggested in [26]. The tube is filled with a caloricaly perfect gas, $\gamma = 1.4$. The left and right states are

- $x \leqslant x_d$

$$\begin{pmatrix} \rho^0(x) \\ \rho^0(x)u^0(x) \\ E^0(x) \end{pmatrix} = \begin{pmatrix} 1 \\ 0 \\ 2.5 \end{pmatrix}$$

- else

$$\begin{pmatrix} \rho^0(x) \\ \rho^0(x)u^0(x) \\ E^0(x) \end{pmatrix} = \begin{pmatrix} 0.125 \\ 0 \\ 0.25 \end{pmatrix} \text{otherwise}$$

The initial position of the diaphragm is uncertain: we set $x_d = 0.5 + 0.05\,\omega$ where the stochastic parameter $\omega \in [-1, 1]$ is described by various pdf (uniform, Gaussian, discontinuous), see figures 1, 2 and 3.

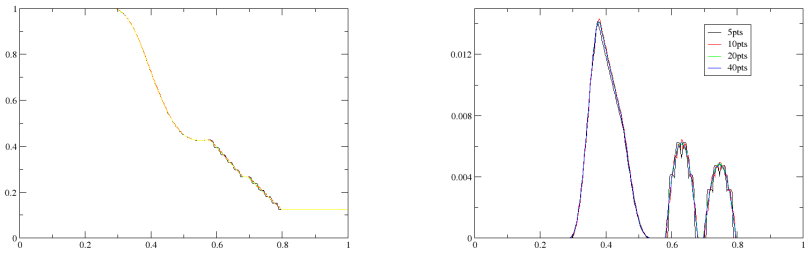

Figure 1: Shock tube with uncertain initial membrane position described by a uniform pdf. Convergence study for the mean density distribution (left) and the standard deviation of the density distribution (right) computed using the stochastic finite volume method.

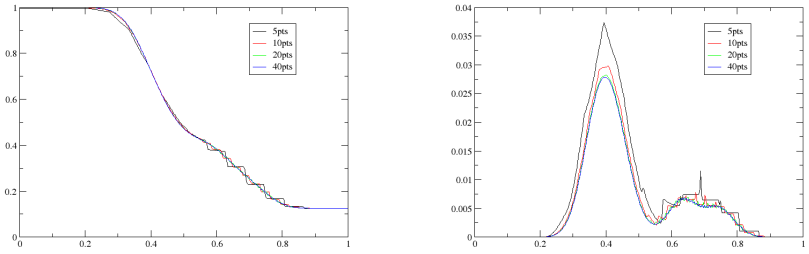

Figure 2: Shock tube with uncertain initial membrane position described by a Gaussian pdf. Convergence study for the mean density distribution (left) and the standard deviation of the density distribution (right) computed using the stochastic finite volume method.

We have run this test case, involving a single random parameter, with the stochastic finite volume method. The results, presented here, use 5, 10, 20 and 40 regularly spaced points in the random space and 200 points the space direction. We can consider that the results are fully converged for this spatial resolution with 20 points. In [26] the results are obtained with a gPC expansion up to polynomial order 11 and 200 points in the space direction.

The second example is a classical RAE2826 airfoil, with the inviscid compressible Euler equations. The uncertainty is on the inflow velocity: we assume $M_\infty = 0.8$, $p_\infty = \frac{1}{\gamma}$ and $U_\infty = 0.8 \pm 2\%$ with a uniform probability law and a Gaussian one with variance 2%. The mesh is unstructured and has about 3, 800 vertices. The numerical scheme uses the RD technology at second order of accuracy, see [50] and [52, 16] for extensions to the Navier-Stokes equation and the turbulent case.

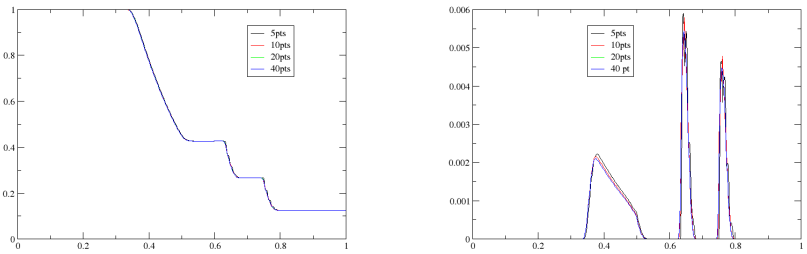

Figure 3: Shock tube with uncertain initial membrane position described by a discontinuous pdf. Convergence study for the mean density distribution (left) and the standard deviation of the density distribution (right) computed using the stochastic finite volume method.

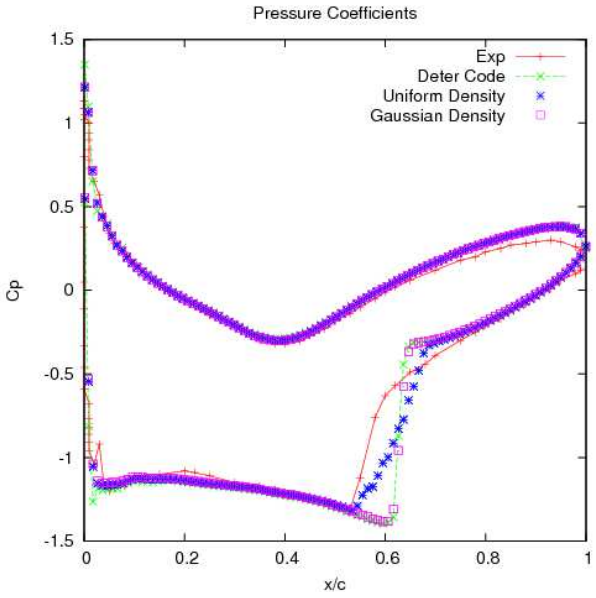

Figure 4: Pressure coefficient for the RAE 2828 case. Experimental data, result of the deterministic case and two UQ simulations are super-imposed.

5.3.2 Uncertain Orszag-Tang vortex.

This test is taken from [66], section 6.2. The system of conservation laws under consideration are the ideal magnetohyrodynamics (MHD) equations of plasma physics. We consider the ideal MHD equations on the two-dimensional domain $[0, 1]^2$ with periodic boundary conditions. The random initial data is an uncertain version of the well-known Orszag-Tang benchmark test problem. We consider a random initial data with 8 sources of uncertainty, namely in the amplitudes of the initial density and pressure, phases of the initial sinusoidal velocity fields and the phases and amplitude of the initial solenoidal magnetic fields. The mean and the variance of the density, computed at time $T = 1.0$ with an MLMC- finite volume method, with 8 levels of resolution, a finest grid of 4096^2 and with 4 samples at the finest level, with the underlying finite volume method using a HLLC Riemann solver, a second-order WENO reconstruction and upwind treatment of the Godunov-Powell source term [21], are shown in figure 5. In this case, one computes a reference solution with the above configuration and calculates the $L^2(\Omega, L^1(D))$ error for both the mean and variance, with MC and MLMC methods (of both first and second order spatio-temporal discretizations). These errors for the mean and variance, are plotted in figures 6 and 7, respectively. They show that the MLMC method is at least $50 - 60$ times faster than the MC method for the mean and $10 - 20$ times faster for the variance, for a given error level. Thus, this justifies the complexity estimates derived in the previous sub-sections, at least for this example.

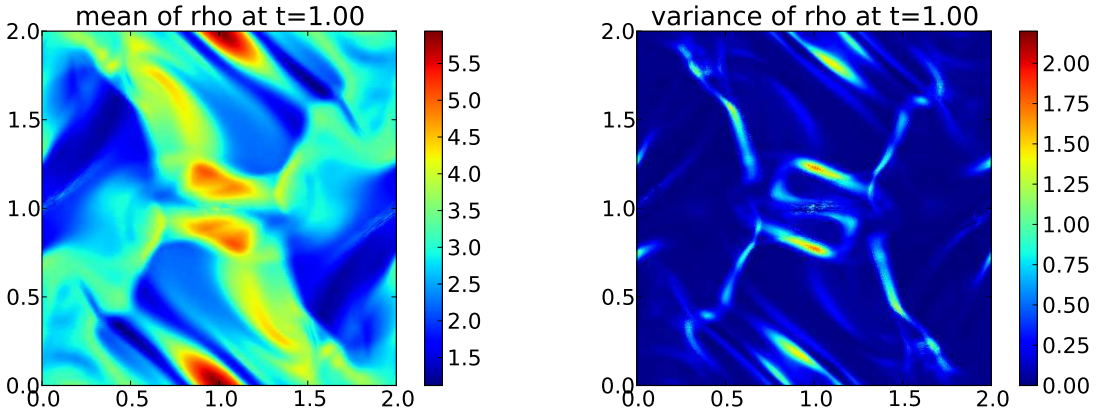

Figure 5: Uncertain Orszag-Tang vortex solution at $t = 1.0$ using MLMC-FVM (8 sources of uncertainty). Left: Mean of density Right: Variance of density. Reproduced from [66]

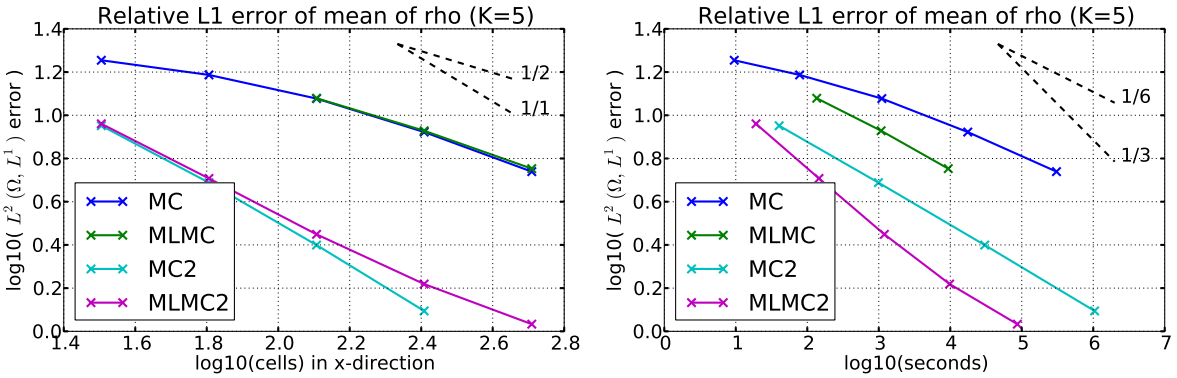

Figure 6: Convergence of mean in the uncertain Orszag-Tang vortex simulation (8 sources of uncertainty). Left: Error vs. Mesh resolution. Right: Error vs. Runtime. Reproduced from [66].

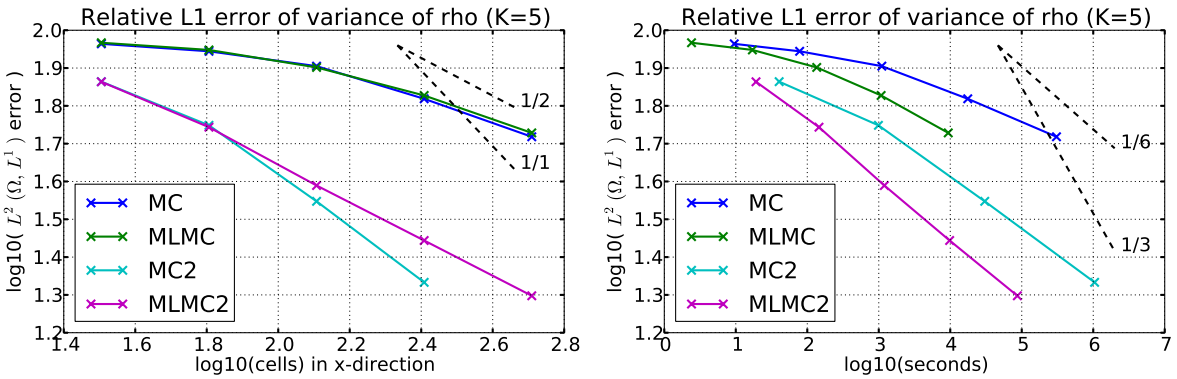

Figure 7: Convergence of variance in the uncertain Orszag-Tang vortex simulation (8 sources of uncertainty).Left: Error vs. Mesh resolution. Right: Error vs. Runtime. Reproduced from [66].

5.3.3 Propagation of acoustic waves in an uncertain medium.

This numerical example is taken from [67]. We consider the acoustic wave equation in three space dimensions, rewritten as a *linear* system of conservation laws. The initial data is taken to be deterministic while the source of uncertainty in this system is the coefficient **c** in (2.10). The coefficient, representing the permeability of the medium, is modeled using a *log-normal Gaussian random field*, represented via a spectral expansion. A single realization of this uncertain coefficient is shown in figure 8 (left). As seen in the figure, the medium is extremely heterogenous with a layered structure and fine microstructures. The resulting random balance law has more than 2 million sources of uncertainty. Incident waves are modeled via a deterministic source term that amounts to specifying a time periodic train of localized incident waves. The mean and variance of the acoustic pressure, computed with an MLMC-finite difference method, with 6 levels of resolution, 8 samples at the finest level, a finest grid of 1024^3, with an underlying second-order high-resolution finite difference method on the a Cartesian grid, are shown in figure 8 (center) and figure 8 (right), respectively. The entire computation took 3 hours on $44,000$ cores. Currently, the MLMC method is only feasible method for computing problems with such high number of sources of uncertainty.

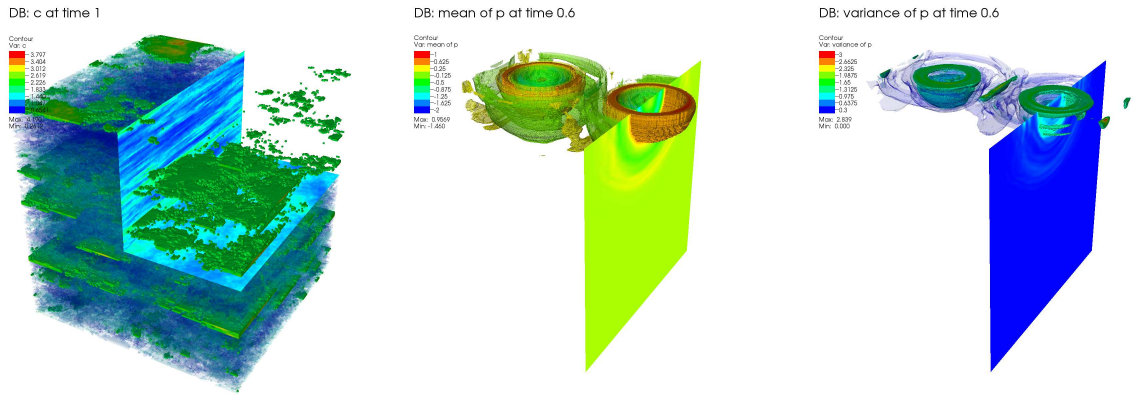

Figure 8: An MLMC-finite difference simulation of propagation of acoustic waves in a layered three-dimensional uncertain medium, modeled by a log-normal Gaussian random field. Left: A single realization of the uncertain rock permeability Center: Mean of acoustic pressure at $T = 0.6$. Right: Variance of acoustic pressure at $T = 0.6$. Figure reproduced from [67].

5.3.4 UQ for the Lituya Bay mega-tsunami.

This numerical example is taken from [12]. The aim is to quantify uncertainty in simulations of the mega-tsunami that was generated by a rockslide (induced in turn by an earthquake) in Lituya Bay, Alaska, in 1958. This event resulted in the largest ever recorded run-up height of 524 m, generated by a tsunami. To simulate this event, one uses a two-layer Savage-Hutter model [70], which is a non-conservative 4×4 hyperbolic system in two space dimensions. The upper layer is water and the lower layer denotes the granular material such as rock or mud. The model contains several source terms, that represent bottom friction, inter-layer friction and momentum exchange between layers. These source terms are based on empirical laws such as the Manning law. The model consists of several undetermined parameters of which, 3, namely the ratio of layer densities, the Coulomb friction angle and the inter-layer friction parameter are very difficult to measure exactly and are only determined upto a probability distribution. Thus, the resulting random system of balance laws has three sources of uncertainty. We plot the mean and variance of the run-up height, at time $T = 39s$, using a MLMC method, with 4 levels of resolution, 16 samples at the finest level, and rectangular grid of 3648×1264 cells at the finest level are shown in figure 9. The underlying spatio-temporal discretization is performed with a first-order path-conservative IFCP scheme [19]. The results show that the standard deviation is approximately 5 percent of the mean, even though the initial standard deviation was 30 percent of the mean. Thus, this simulation is fairly unsensitive to the uncertain parameters. The entire simulation was completed is approximately 1 hour on a Tesla K20 GPU. We observed a gain of efficiency of approximately 10 over a corresponding Monte Carlo simulation.

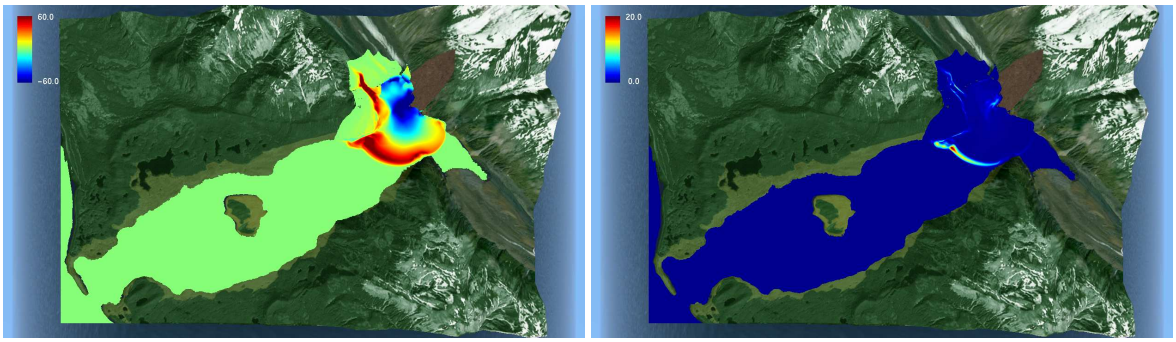

Figure 9: An MLMC-finite volume simulation of the run-up height of the Lituya Bay mega tsunami . Left: Mean run-up height at $T = 39s$. Right: Variance of run-up height at $T = 39s$. Figure reproduced from [12].

5.3.5 A random Kelvin-Helmholtz problem.

The last numerical example is taken from a recent paper [76] and the MLMC computations are presented in a forthcoming paper [39]. We consider the compressible Euler equations in the two-dimensional domain $[0, 1]^2$ with periodic boundary conditions. The uncertainty arises due to the initial data being a (very small) random perturbation of the classic Kelvin-Helmholtz problem, see [76], with 20 sources of uncertainty in the initial data. The mean and variance of the density, computed with a Monte Carlo method, on a Cartesian 1024^2 grid and with 400 MC samples are shown in figure 10 (Top Row). The underlying finite volume scheme is the third-order entropy stable TeCNO scheme of [80]. Surprisingly for this test case, the variance of the solution is at least three orders of magnitude higher than the variance of the initial data. This amplification of variance is due to the generation of structures at smaller and smaller scales, when the shear flow interacts with the contact discontinuity. In this particular case, the MLMC method provides *no gain* in computational efficiency over the standard Monte Carlo method. This is depicted in figure 10 (Bottom row, Left), where the L^1 difference in the mean of the density, computed with the MLMC and MC methods, at the same grid resolution for the finest grid and the same number of samples at the finest grid resolution of MLMC, with respect to an MC reference solution computed with 1024 samples, is compared. The results show that error due to MLMC is comparable to the error due to the MC calculation, provided that the number of samples at the finest grid level of the MLMC calculation is the same as the number of MC samples. Thus, in this case, the coarse levels of the MLMC method do not increase the accuracy of the computation and are redundant. Given this observation, it is clear that the error estimate (5.8) cannot hold for this particular example. In fact, even the error estimate (5.2) for the underlying spatio-temporal discretization, does not hold for this example.

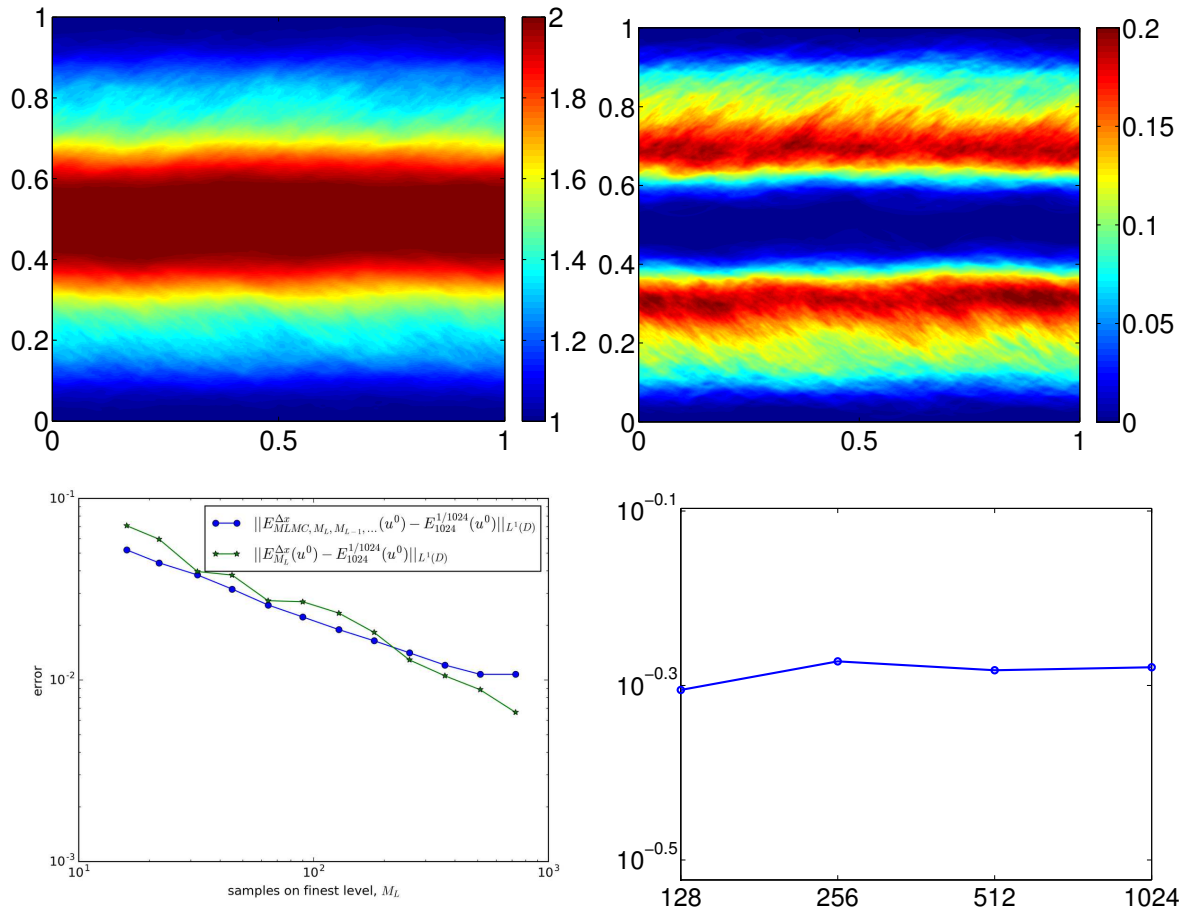

Figure 10: UQ for the random Kelvin-Helmholtz problem. Top Row: Density at time $T = 2$ computed with MC method and TeCNO3 scheme with algorithm proposed in [76] Left: Mean, Right: Variance (Reproduced from [76]. Bottom Row Left: Comparison between MC and MLMC method with respect to error in mean of the density with respect to a reference solution (Reproduced from [39]. Bottom Right: Lack of convergence for a single sample for the density (reproduced from [76].

We see this from figure 10 (Bottom row, Right) where the difference in L^1 between two successive mesh resolutions for a single sample is shown. This figure shows that the error remains constant with respect to resolution and the underlying finite volume scheme does not converge for this particular test case. It was also shown in [39] that even weaker convergence bounds, such as the variance of the difference between successive resolutions, does not hold for this particular problem, as structures at even smaller scales are generated upon mesh refinement.

6 Measure-valued and Statistical solutions.

It is interesting to note that the Monte Carlo method converges for the previous numerical experiment, as shown in figure 10 (bottom left), even though the underlying spatio-temporal discretization may not converge in L^1, as shown in figure 10 (bottom right). The reason for this observed convergence was provided in recent papers [76, 78], see also [28] and references therein. There, the authors proved that a Monte Carlo based algorithm, together with an entropy stable scheme such as the TeCNO scheme of [80], converges to an *entropy measure valued solution* of the underlying system of conservation laws. Measure valued solutions were proposed by [60] and are in fact *Young measures* i.e, space-time parametrized probability measures on the phase space $\mathbb{R}^N$ of (1.1). They can be interpreted as point probability density functions. Furthermore, entropy measure valued solutions are consistent with the weak solution (1.2) and with the entropy inequality. Existence of measure-valued solutions was shown in [76, 78] and references therein, by proving convergence of a Monte Carlo based ensemble averaging algorithm. Moreover, the convergence theorem imposed some properties on spatial discretizations as necessary conditions for convergence. These properties are satisfied by arbitrarily high-order entropy stable schemes of [80] and the fully discrete shock capturing space-time Discontinuous Galerkin methods of [7]. A large number of numerical experiments were presented in [76, 78], which demonstrated that statistical quantifies of interest, such as the mean, variance and point-pdf, can converge (with increasing grid resolution and number of Monte Carlo samples), even if individual realizations do not converge, such as in the previous numerical experiment. Furthermore, the computations of [76] also demonstrated that the measure-valued solution may not be atomic even if the initial data is an *atomic young measure*, concentrated on a L^1 function. *Thus, there seems to be no such thing as a fully deterministic version of multi-dimensional systems of conservation (balance) laws and the hitherto deterministic initial value problem for* (1.1)*, is in fact a problem in uncertainty quantification (UQ).*

Measure-valued solutions exist for all times and are able to represent limits of numerical approximation of systems of conservation (balance) laws (1.1). They also serve as an UQ framework within which the random initial data is represented as a Young measure (or point probability distribution). However, measure-valued solutions are not necessarily unique, particularly when the initial data is non-atomic. This holds true even for scalar conservation laws. Thus, one needs to augment measure-valued solutions with additional constraints in order to recover uniqueness. One such attempt has been made recently in [77]. In this paper, the authors propose the concept of *statistical solutions* of systems of conservation laws as a suitable solution paradigm as well as an UQ framework. Statistical solutions are time-parametrized probability measures on a L^p function space. By a novel equivalence property shown in [77], this probability measure on an infinite-dimensional space is equivalent to a hierarchy of Young measures on finite-dimensional tensor product domains. This hierarchy is termed a *correlation measure* and its k-th member, termed a *k-point correlation marginal* is a Young measure that encodes information about correlations (joint probabilities) of the underlying functions at k distinct points of the spatial domain. The one-point correlation marginal is the classical Young measure. Certain moments of the correlation measures, the so-called correlation functions, determine the underlying probability measure on L^p uniquely. Hence, the time-evolution of statistical solutions is specified by infinite family of coupled PDEs, each evolving a correlation function. Well-posedness of *entropy statistical solutions* was shown in [77]. It turns out that the same Monte Carlo ensemble averaging algorithm, proposed in [76], also converges, under sufficient conditions, to a statistical solution of the underlying system. This will be shown in a forthcoming paper [75]. Thus, statistical solutions may provide a suitable solution framework for multi-dimensional systems of conservation laws.

Statistical solutions do provide an alternative paradigm for UQ. Instead of modeling the uncertainty in initial data, sources, coefficients etc in terms of random fields, one can instead define a probability measure on the underlying L^p space by taking the *law* of the random field. Thus, the initial data will be a probability measure on L^p and will evolve in the form of a statistical solution. The advantages of this approach over that of random fields and random entropy solutions are

i. The modeling of uncertainty of initial inputs, and solutions, is completely independent of any parametrization.

Random fields force one to pick a particular parametrization whereas just specifying their law provides for a more robust and parameter independent approach. The same is true for the resulting statistical solutions.

ii. Statistical solutions can exist (globally in time) even if there is no data to solution operator in L^p spaces. Such a global existence result may not be possible for random entropy solutions as they rely on the existence of data to solution operators, which may not exist for multi-dimensional system of conservation laws [76].

iii. Convergent Monte Carlo approximations of statistical solutions are possible. On the other hand, it is very difficult to obtain rigorous convergence results for any kind of approximation of random entropy solutions for multi-dimensional systems of conservation (balance) laws, in view of the fact that error estimates for the deterministic problem, such as (5.2), that underly any convergence analysis, do not hold.

7 Conclusion and perspectives.

Inputs to any system of balance laws, such as the initial data, fluxes, coefficients, source terms and boundary conditions, are obtained through measurement. Any measurement process leads to some degree of uncertainty in the input. This input uncertainty propagates into the solution and needs to be modeled and computed efficiently. Moreover, systems of conservation (balance) laws, particularly in several space dimensions, might require a probabilistic solution paradigm, even if the inputs are determined exactly. This is largely due to the chaotic behavior of unstable and turbulent flows. Thus, uncertainty quantification (UQ) is a very important aspect for hyperbolic PDEs, from the perspective of applications and in order to answer the fundamental question of well-posedness of these systems.

The broad area of UQ for hyperbolic systems of balance laws has witnessed a very large amount of research activity in recent years. In this article, we have reviewed some important themes within UQ for hyperbolic problems. The most popular current framework for modeling uncertain inputs (and solutions) is that of random fields and random entropy solutions. Input uncertainty is expressed in terms of finite number of parameters, for instance determined by the underlying physics. An alternative approach consists of performing a Karhunen-Loeve expansion or other spectral expansions, and then truncating to a finite sum, based on the decay of the Karhunen-Loeve eigenvalues. In either case, the probability space could be very high dimensional, posing an enormous challenge to the design of efficient algorithms for UQ. Another vexing problem stems from the fact that discontinuities in space-time (which are inevitable in nonlinear hyperbolic problems) propagate into the random space. Consequently, there is no regularity of the random entropy solution with respect to uncertain parameters. This lack of regularity impedes the adaptation of efficient algorithms from elliptic and parabolic problems to UQ for hyperbolic problems [58].

Nevertheless, several methods for UQ, in the context of hyperbolic problems, have been proposed. We have described the stochastic Galerkin method, based on generalized polynomial chaos. A direct version of this method results in systems that may not necessarily be hyperbolic. A gPC expansion in terms of entropy variables (or cleverly designed splittings) can alleviate this problem. However, stochastic Galerkin methods are currently restricted to problems with low to moderate number of uncertain parameters, due to the intrinsic lack of regularity, that prevents one from using hierarchical data representations. Furthermore, stochastic Galerkin methods are *intrusive*.

A non- or semi-intrusive alternative is proved by the stochastic collocation methods. Lack of regularity inhibits a direct adaptation of stochastic collocation methods, developed for elliptic and parabolic problems. A promising variant is provided by the stochastic collocation finite volume methods reviewed here. These methods use non-oscillatory piecewise polynomial basis functions and are adapted to the presence of discontinuities in the random space. However, the use of compression techniques such as sparse grids and other hierarchical representations is inhibited by the lack of regularity. Thus, stochastic collocation finite volume methods are able to only handle low to moderate number of uncertain parameters currently. However, some spatial and parametric regularity can be obtained in several cases, see the so-called probabilistic shock profiles analyzed in [13, 69].

An alternative class of methods are of the statistical sampling or Monte Carlo type. These methods are robust, totally non-intrusive and trivial to parallelize. The performance of Monte Carlo methods is also independent of the number of uncertain parameters. However, these methods converge rather slowly with respect to the number of samples. This slow convergence and resultant high computational cost motivate the design of Monte Carlo variants. A promising framework is that of Multi-level Monte Carlo (MLMC) methods, in which the problem is approximated on a sequence of spatio-temporal mesh resolutions. A large number of samples are drawn on the coarse meshes

while a very small number of samples are drawn on the fine mesh resolutions. The MLMC estimator is based on *details* i.e, difference of the solution on successive meshes. If the underlying spatio-temporal discretization of the deterministic problem converges in L^p, then one can prove that the MLMC method will be more computationally efficient than the Monte Carlo method. This is also demonstrated by a large number of numerical experiments that show that the MLMC method is indeed, orders of magnitude, faster than the corresponding MC computation. Moreover, MLMC can handle problems with very large number of sources of uncertainty. We have presented an example with more than 2 million sources of uncertainty. Augmented with novel algorithms for static or dynamic load balancing on very large scale massively parallel implementations, MLMC can be a method of choice for a large number of UQ problems, arising in science and engineering.

However, there are problems for which MLMC is no better than the underlying MC method. These are problems that involve the presence of a very large number of spatial and/or temporal scales, that cannot be resolved even on the finest of available mesh resolutions. In fact, the underlying inviscid deterministic problem is not necessarily well-posed for these unstable and turbulent flows. On the other hand, one can resort to weaker solution concepts, such as measure valued and statistical solutions, for these problems. Statistical solutions are an attractive framework as one-point statistics (young measures) are augmented by multi-point spatial correlations. Thus, they can serve as a paradigm for uncertainty quantification for unstable and turbulent flows. Moreover, one can show convergence of Monte Carlo algorithms to statistical solutions. However, these concepts are in the very early stages of development and the jury is still out on them. On the other hand, they can motivate the design of Monte Carlo variants such as quasi-Monte Carlo, ANOVA decompositions [83] or deterministic algorithms for computing statistical solutions.

We have reviewed only the problem of uncertainty propagation or forward UQ in this article. Inverse problems, particularly in the Bayesian framework [8] are very important in practice but hardly investigated in the context of hyperbolic problems. One example is [34] where one determines the inflow conditions for an hypersonic vehicle from heat flow and pressure measurement on the wall of the vehicle. Similarly, model order reduction is a related fundamental issue that is only seeing the beginning of a research program [51]. We conclude by stating that the subject of UQ for hyperbolic problems is still in its infancy and will see substantial development in the coming years.

Acknowledgements

R. A. acknowledges the partial support of the Swiss National Foundation grant 200021-153604. SM acknowledges partial support from ERC STG 306279 SPARCCLE.

References

[1] S. Gottlieb and C. W. Shu and E. Tadmor. High order time discretizations with strong stability property. *SIAM Review*, 43:89–112, 2001.

[2] A. Barth and Ch. Schwab and N. Zollinger. Multilevel MC Method for Elliptic PDEs with Stochastic Coefficients. *Numerische Mathematik*, 119(1):123–161, 2011.

[3] A. Chertock and S. Jin and A. Kurganov. A well-balanced operator splitting based stochastic Galerkin method for the one-dimensional Saint-Venant system with uncertainty. Preprint, 2015.

[4] A. Chertock and S. Jin and A. Kurganov. An operator splitting based stochastic Galerkin method for the one-dimensional compressible Euler equations with uncertainty. Preprint, 2015.

[5] A. Cohen and R. DeVore and C. Schwab. Convergence rates of best N-term Galerkin approximations for a class of elliptic sPDEs. *J. FoCM*, pages 615–646, 2010.

[6] A. Harten and B. Engquist and S. Osher and S. R. Chakravarty. Uniformly high order accurate essentially non-oscillatory schemes. *J. Comput. Phys.*, pages 231–303, 1987.

[7] A. Hiltebrand and S. Mishra. Entropy stable shock capturing streamline diffusion space-time discontinuous Galerkin (DG) methods for systems of conservation laws. *Numer. Math.*, 126(1):103–151, 2014.

[8] A. M. Stuart. Inverse problems: a Bayesian perspective. *Acta Numerica*, 19:451–559, 2010.

[9] R. Abgrall. Residual distribution schemes: Current status and future trends. *Comput. Fluids*, 35(7):641–669, 2006.

[10] B. Cockburn and C-W. Shu. TVB Runge-Kutta local projection discontinuous Galerkin finite element method for conservation laws. II. General framework. *Math. Comput.*, 52:411–435, 1989.

[11] C. Johnson and A. Szepessy and P. Hansbo. On the convergence of shock capturing streamline diffusion finite element methods for hyperbolic conservation laws. *Math. Comp.*, 54:107–129, 1990.

[12] C. Sanchez-Linares and M. de la asuncion and M. Castro and S. Mishra and J. Sukys. Multi-level Monte Carlo finite volume method for shallow water equations with uncertain parameters applied to landslides-generated tsunamis,. *Appl. Math. Modeling*, 39(23-24):7211–7226, 2015.

[13] C. Schwab and S. Tokareva. High order approximation of probabilistic shock profiles in hyperbolic conservation laws with uncertain initial data. *M2AN Mathematical Modelling and Numerical Analysis*, 47:807–835, 2013.

[14] C. W. Shu and S. Osher. Efficient implementation of essentially non-oscillatory schemes - II. *J. Comput. Phys.*, 83(1):32–78, 1989.

[15] Constantine M. Dafermos. *Hyperbolic Conservation Laws in Continuum Physics*. Springer Verlag, 2005. 2nd Edition.

[16] D. de Santis. High-order linear and non-linear residual distribution schemes for turbulent compressible flows. *Computer Methods in Applied Mechanics and Engineering*, 285:1–31, 2015.

[17] D. Xiu and G. E. Karniadakis. The Wiener-Askey polynomial chaos for stochastic differential equations. *SIAM J. Sci. Comp.*, 24(2):619–644, 2002.

[18] D. Xiu and J. S. Hesthaven. High-order collocation methods for differential equations with random inputs. *SIAM J. Sci. Comput.*, 27:1118–1139, 2005.

[19] E.D. Fernández-Nieto and M.J. Castro C. and Parés. On an Intermediate Field Capturing Riemann Solver Based on a Parabolic Viscosity Matrix for the Two-Layer Shallow Water System. *J. Sci. Comput.*, 48(1-3), 2011.

[20] Edwige Godlewski and Pierre A. Raviart. *Hyperbolic Systems of Conservation Laws.* Mathématiques et Applications. Ellipse, 1991.

[21] F. Fuchs and A. D. McMurry and S. Mishra and N. H. Risebro and K. Waagan. Approximate Riemann solver based high-order finite volume schemes for the Godunov-Powell form of ideal MHD equations in multi-dimensions. *Comm. Comput. Phys.*, 9:324–362, 2011.

[22] F. Müller. *Stochastic methods for uncertainty quantification in subsurface flow and transport problems.* PhD thesis, ETH, 2014.

[23] F. Müller and P. Jenny and D.W. Meyer. Multilevel Monte Carlo for two Phase Flow and Buckley-Leverett Transport in Random Heterogeneous Porous Media. *J. Comput. Phys.*, 250(1):685–702, 2013.

[24] G. Lin and C.H. Su and G. E. Karniadakis. The stochastic piston problem. *PNAS*, 101:15840–15845, 2004.

[25] G. Lin and C.H. Su and G.E. Karniadakis. Predicting shock dynamics in the presence of uncertainties. *J. Comput. Phys.*, 217:260–276, 2006.

[26] G. Poette and B . Després and D. Lucor. Uncertainty quantification for systems of conservation laws. *J. Comput. Phys.*, 228:2443–2467, 2009.

[27] H. Bijl and D. Lucor and S. Mishra and Ch. Schwab, editor. *Uncertainty quantification in computational fluid dynamics*, volume 92 of *Lecture notes in computational science and engineering*. Springer, 2014.

[28] H. Lim and Y. Yu and J. Glimm and X. L. Li and D. H. Sharp. Chaos, transport and mesh convergence for fluid mixing. *Act. Math. Appl. Sin*, 24(3):355–368, 2008.

[29] Harten, Ami. Multiresolution algorithms for the numerical solution of hyperbolic conservation laws. *Communications on Pure and Applied Mathematics*, 48(12):1305–1342, 1995.

[30] I. Müller and T. Ruggeri. Rational extended thermodynamics. *Springer tracts in natural philosophy*, 1998.

[31] J. A. S. Witteveen and G. Iaccarino. Essentially non-oscillatory stencil selection and subcell resolution in uncertainty quantification. In *Uncertainty Quantification in Computational Fluid Dynamics*, volume 92 of *Lecture Notes in Computational Science and Engineering* , pages 295–333, 2013.

[32] J. Tryoen and O. Le Maitre and M. Ndjinga and A. Ern. Intrusive projection methods with upwinding for uncertain non-linear hyperbolic systems. *J. Comput. Physics*, 229:6485–6511, 2010.

[33] J. Tryoen and O. Le Maitre and M. Ndjinga and A. Ern. Roe solver with entropy corrector for uncertain hyperbolic systems. *J. Comput. Phys.*, 235:491–506, 2010.

[34] J. Tryoen and P. Congedo and R. Abgrall and T. Magin and N. Villedieu. Sensitivity analysis and characterization of the uncertain input data for the EXPERT vehicle. *AIAA Journal*, 52:2190–2197, 2014.

[35] J. Šukys. Adaptive load balancing for massively parallel multi-level Monte Carlo solvers. In *PPAM2013, Part I*, number 8384 in LNCS, pages 47–56. Springer, 2014.

[36] J. Šukys. *Robust multi-level Monte Carlo Finite Volume methods for systems of hyperbolic conservation laws with random input data*. PhD thesis, ETH, 2014.

[37] J. Šukys and Ch. Schwab and S. Mishra. Multi-Level Monte Carlo Finite Difference and Finite Volume methods for stochastic linear hyperbolic systems. In *MCQMC 2012*, Proceedings in Mathematics & Statistics, pages 649–666. Springer, 2013.

[38] J. Šukys and S. Mishra and Ch. Schwab. Static load balancing for multi-level Monte Carlo finite volume solvers. In *PPAM 2011, Part I*, volume 7203 of *Lecture Notes in Computational Sciences*, pages 245–254. Springer Verlag, 2012.

[39] K.O. Lye. Multi-level Monte Carlo methods for computing measure-valued solutions of hyperbolic conservation laws. *in preparation*, 2016.

[40] M. Ricchiuto and A. Bollerman. Stabilized residual distribution for shallow water simulations. *J. Comput. Phys.*, 228:86–113, 2009.

[41] M. Ricchiuto and P.M. Congedo and G. Geraci and R. Abgrall. Uncertainty propagation in shallow water long wave run up simulations. In *First International Conference on Frontiers of Comput. Physics: Modelling the Earth System*. Elsevier, 2012. Boulder, CO.

[42] M.B. Giles. Multilevel Monte Carlo path simulation. *Oper. Res.*, 56:607–617, 2008.

[43] M.B. Giles. Multilevel Monte Carlo methods. *Acta Numerica*, 24:259–328, 2015.

[44] N. Collier and A. L. Haji-Ali and F. Nobile and E. von Schwerin and R. Tempone. A continuation multilevel Monte Carlo algorithm. *BIT Num. Math.*, 55(2):399–432, 2015.

[45] N. Wiener. The homogeneous chaos. *Amer. J. Math.*, 60:897–936, 1938.

[46] P.G. Ciarlet and P.A. Raviart. General Lagrange and Hermite interpolation in R^n with applications to finite element methods. *Arch. Ration. Mech. Anal.*, 46:177–199, 1972.

[47] Q. Y. Chen and D. Gottlieb and J. S. Hesthaven. Uncertainty analysis for steady flow in a dual throat nozzle. *J. Comput. Phys.*, 204:378–398, 2005.

[48] R. Abgrall. On essentially non-oscillatory schemes on unstructured meshes: Analysis and implementation. *J. Comput. Phys.*, 114(1):45–58, 1994.

[49] R. Abgrall. A simple, flexible and generic deterministic approach to uncertainty quantification in non-linear problems. Technical report, Inria, 2008.

[50] R. Abgrall and A. Larat and M. Ricchiuto. Construction of very high order residual distribution schemes for steady inviscid flow problems on hybrid meshes. *J. Comput. Phys.*, 230(11):4103–4136, 2011.

[51] R. Abgrall and D. Amsallem and R. Crisovan. Robust model reduction by L^1-norm minimization and approximation via dictionaries: application to nonlinear hyperbolic problems. *Adv. Mod. Sim. Engg. Sci.*, 3(1), 1–16 2016.

[52] R. Abgrall and D. de Santis. Linear and non-linear high order accurate residual distribution schemes for the discretization of the steady compressible Navier-Stokes equations. *J. Comput. Phys.*, 283:329–359, 2015.

[53] R. Abgrall and P. Congedo. A semi-intrusive deterministic approach to uncertainty quantification in non-linear fluid flow problems. *J. Comput. Phys.*, 235:828–845, 2013.

[54] R. Abgrall and P. Congedo and C. Corre and S. Galera. A simple semi-intrusive method for uncertainty quantification of shocked flows, comparison with non-intrusive polynomial chaos method. In *V Conference on Computational Fluid Dynamics, ECCOMAS CFD*. ECCOMAS, 2010. Lisbon, Portugal, 14-17 June 2010.

[55] R. Abgrall and P.M. Congedo and G. Geraci. A one-time truncate and encode multiresolution stochastic framework. *J. Comput. Phys.*, 257(A):19–56, 2014.

[56] R. Abgrall and P.M. Congedo and G. Geraci and M.G. Rodio. Stochastic discrete equation method (sDEM) for two phase flows. *J. Comput. Phys.*, 299:281–306, 2015.

[57] R. Abgrall and Thomas Sonar. On the use of Mühlbach expansions in the recovery step of ENO methods. *Numer. Math.*, 76(1):1–25, 1997.

[58] R. Ghanem and D. Higdon and H. Owhadi, editor. *Handbook of uncertainty quantification*. Springer, 2016.

[59] R. H. Cameron and W. T. Martin. The orthogonal development of non-linear functionals in series of Fourier-Hermite functionals. *Ann. Math.*, 48:385–392, 1947.

[60] R. J. DiPerna. Measure-valued solutions to conservation laws. *Archive for Rational Mechanics and Analysis*, 88:223–270, 1985.

[61] R.A. LeVeque. *Numerical Solution of Hyperbolic Conservation Laws*. Cambridge University Press, 2005.

[62] S. Heinrich. Multilevel Monte Carlo methods. In *Large-scale scientific computing, Third international conference LSSC 2001, Sozopol, Bulgaria*, volume 2170 of *Lecture Notes in Computer Science*, pages 58–67. Springer Verlag, 2001.

[63] S. Mishra and C. Schwab. Sparse tensor multi-level Monte Carlo finite volume methods for hyperbolic conservation laws with random initial data. *Math. Comput.*, 81(180):1979–2018, 2012.

[64] S. Mishra and Ch. Schwab and J. Šukys. Multi-level Monte Carlo finite volume methods for nonlinear systems of conservation laws in multi-dimensions. *J. Comput. Phys.*, 231(8):3365–3388., 2012.

[65] S. Mishra and Ch. Schwab and J. Šukys. Multi-level Monte Carlo Finite Volume methods for shallow water equations with uncertain topography in multi-dimensions. *SIAM J. Sci. Comput.*, 34(6):B761–B784, 2012.

[66] S. Mishra and Ch. Schwab and J. Šukys. Monte Carlo and multi-level Monte Carlo finite volume methods for uncertainty quantification in nonlinear systems of balance laws. In *Uncertainty Quantification in Computational Fluid Dynamics.*, volume 92 of *Lecture Notes in Computational Science and Engineering Volume*, pages 225–294, 2013.

[67] S. Mishra and Ch. Schwab and J. Šukys. Multi-Level Monte Carlo Finite Volume methods for uncertainty quantification of acoustic wave propagation in random heterogeneous layered medium. *J. Comput. Phys.*, 312:192–217, 2016.

[68] S. Mishra and N.H. Risebro and Ch. Schwab and S. Tokareva. Numerical solution of scalar conservation laws with random flux functions. *SIAM/ASA Jl. Uncertainty Quantification.*, 4(1):552–591, 2016.

[69] S. Tokareva. *Numerical solution of conservation laws with random flux*. PhD thesis, ETH Zürich, 2013.

[70] S.B. Savage and K. Hutter. The motion of a finite mass of granular material down a rough incline. *J. Fluid. Mech.*, 199:177–215, 1989.

[71] T. J. Barth and P. O. Frederickson. Higher order solution of the euler equations on unstructured grids using quadratic reconstruction. AIAA paper 90-0013, January 1990.

[72] T.J. Barth. On the propagation of statistical model parameter uncertainty in CFD calculations. *Theo. Comp. Fluid. Dynamics*, 26:435–457, 2012.

[73] T.J. Barth. Non-intrusive uncertainty propagation with error bounds for conservation laws containing discontinuities. In *Uncertainty Quantification in Computational Fluid Dynamics.*, volume 92 of *Lecture Notes in Computational Science and Engineering*, pages 1–58, 2013.

[74] T.J.R. Hughes and M. Mallet. A new finite element formulation for CFD III: the generalized streamline operator for multidimensional advective-diffusive systems. *Comp. Meth. Appl. Mech. Engrg.*, 58:305–328, 1986.

[75] U. S. Fjordholm and R. Käppeli and K. O. Lye and S. Mishra. Statistical solutions of hyperbolic conservation laws III: Numerical approximation for multi-dimensional systems. in preparation, 2016.

[76] U. S. Fjordholm and R. Käppeli and S. Mishra and E. Tadmor. Construction of approximate entropy measure-valued solutions for hyperbolic systems of conservation laws. *J. FoCM*, 2016. to appear.

[77] U. S. Fjordholm and S. Lanthaler and S. Mishra. Statistical solutions of hyperbolic conservation laws I: Foundations. Available from ArXiv:1605.05960, 2016.

[78] U. S. Fjordholm and S. Mishra and E. Tadmor. On the computation of measure-valued solutions. *Acta Numerica*, 25:567–679, 2016.

[79] U.S. Fjordholm and S. Mishra and E. Tadmor. Well-balanced, energy stable schemes for the shallow water equations with varying topology. *J. Comput. Phys.*, 230:5587–5609, 2011.

[80] U.S. Fjordholm and S. Mishra and E. Tadmor. Arbitrarily high-order order accurate essentially non-oscillatory entropy stable schemes for systems of conservation laws. *SIAM J. Numer. Anal.*, 50(2):544–573, 2012.

[81] X. Ma and N. Zabaras. An adaptive hierarchical sparse grid collocation algorithm for the solution of stochastic differential equations. *J. Comput. Phys.*, 228:3084–3113, 2009.

[82] X. Wan and G. E. Karniadakis. Long-term behaviour of polynomial chaos in stochastic flow simulations. *Comput. Meth. Appl. Mech. Engg*, 195:5582–5596, 2006.

[83] X. Yang and M. Choi and G. Lin and G.E. Karniadakis. Adaptive ANOVA decomposition of stochastic incompressible and compressible flows. *J. Comput. Phys.,*, 231:1587–1614, 2012.